

JET PROPULSION LABORATORY

SIRTF IPF REPORT

JPL ID602095

December 4, 2003

**SIRTF INSTRUMENT POINTING FRAME  
KALMAN FILTER EXECUTION SUMMARY**

IPF RUN NUMBER: 602095

REPORT TYPE: IOC EXECUTION (FINE)

PRIME FRAME: MIPS\_24um\_center (95)

INFERRRED FRAMES: (96) (99) (100) (103) (104)

**IPF TEAM**

Autonomy and Control Section (345)

Jet Propulsion Laboratory

California Institute of Technology

4800 Oak Grove Drive

Pasadena, CA 91109

# Contents

<b>1 IPF EXECUTION SUMMARY</b>	<b>5</b>
<b>2 IPF INPUT FILE HISTORY</b>	<b>9</b>
<b>3 IPF EXECUTION RESULTS</b>	<b>12</b>
3.1 IPF EXECUTION OUTPUT PLOTS . . . . .	12
3.2 IPF OUTPUT DATA (IF MINI FILE) . . . . .	38
3.3 IPF EXECUTION LOG . . . . .	42
<b>4 COMMENTS</b>	<b>45</b>

## List of Figures

1.1 A-priori and a-posteriori IPF frames . . . . .	5
1.2 A-priori and a-posteriori IPF frames (ZOOMED) . . . . .	8
2.1 Scenario Plot . . . . .	9
2.2 Attitude file edit history . . . . .	10
2.3 Centroid file edit history . . . . .	10
2.4 Oriented PixelCoords of Centroid Meas. Edited Centroids . . . . .	11
3.1 TPF coords of measurements and a-priori predicts . . . . .	14
3.2 Oriented PixelCoords of measurements and a-priori predicts . . . . .	14
3.3 Oriented (W,V) PixelCoords of A-Priori Prediction Error Quiver Plot . . . . .	15
3.4 A-priori prediction error (Science Centroids) . . . . .	15
3.5 Oriented PixelCoords of measurements and a-priori predicts (PCRS only) . . . . .	16
3.6 Oriented PixelCoords of measurements and a-priori predicts (Zoomed, PCRS only) . .	16
3.7 Oriented (W,V) PixelCoords of A-Priori PCRS Prediction Error Quiver Plot . . . . .	17
3.8 A-priori PCRS prediction error . . . . .	17
3.9 IPF execution convergence, chart 1 . . . . .	18
3.10 IPF execution convergence, chart 2 . . . . .	18
3.11 Parameter uncertainty convergence . . . . .	19
3.12 IPF parameter symbol table . . . . .	19
3.13 KF parameter error sigma plots . . . . .	20
3.14 LS parameter error sigma plot . . . . .	20

3.15 KF and LS parameter error sigma plot . . . . .	21
3.16 Oriented Pixel Coords of meas. and a-posteriori predicts . . . . .	22
3.17 Oriented Pixel Coords of meas. and a-posteriori predicts (attitude corrected) . . . . .	22
3.18 KF innovations with (o) and w/o (+) attitude corrections . . . . .	23
3.19 Histograms of science a-posteriori residuals (or innovations) . . . . .	23
3.20 A-Posteriori Science Centroid Prediction Error Quiver (Att. Cor.) . . . . .	24
3.21 Normalized A-Posteriori Science Centroid Prediction Errors . . . . .	24
3.22 KF innovations with (o) and w/o (+) attitude corrections (PCRS) . . . . .	25
3.23 Histograms of PCRS a-posteriori residuals (or innovations) . . . . .	25
3.24 A-posteriori PCRS Prediction Summary . . . . .	26
3.25 A-posteriori PCRS Prediction (PCRS 1 Only) . . . . .	27
3.26 A-posteriori PCRS Prediction (PCRS 2 Only) . . . . .	27
3.27 A-Posteriori PCRS Prediction Errors Quiver (Att. Cor.) . . . . .	28
3.28 Normalized A-Posteriori PCRS Prediction Errors . . . . .	28
3.29 W-axis KF innovations and 1-sigma bound . . . . .	29
3.30 V-axis KF innovations and 1-sigma bound . . . . .	29
3.31 Array plot with (solid) and w/o (dashed) optical distortion corrections . . . . .	30
3.32 Optical Distortion Plot: total (x5 magnification) . . . . .	30
3.33 Optical Distortion Plot: constant plate scales (x5 magnification) . . . . .	31
3.34 Optical Distortion Plot: linear plate scale (x5 magnification) . . . . .	31
3.35 Optical Distortion Plot: gamma terms (x5 magnification) . . . . .	32
3.36 Scan Mirror Chops . . . . .	32
3.37 IPF Frame Reconstruction . . . . .	33
3.38 Center Pixel Reconstruction . . . . .	33
3.39 Estimated attitude corrections (Body frame) . . . . .	34
3.40 Estimated attitude error sigma plot (Body frame) . . . . .	34
3.41 Thermo-mechanical boresight drift (equiv. angle in (W,V) coords) . . . . .	35
3.42 Thermo-mechanical boresight drift (equiv. angle in Body frame) . . . . .	35
3.43 Gyro drift bias contribution (equiv. rate in (W,V) coords) . . . . .	36
3.44 Gyro drift bias contribution (equiv. angle in (W,V) coords) . . . . .	36
3.45 Gyro drift bias contribution (equiv. angle in Body frame) . . . . .	37

# List of Tables

1.1	IPF filter input files . . . . .	6
1.2	IPF filter execution configuration . . . . .	6
1.3	IPF filter execution mask vector assignment . . . . .	6
1.4	IPF calibration error summary ([arcsec], 1-sigma, radial) . . . . .	7
1.5	Science measurement prediction error summary (1-sigma) . . . . .	7
1.6	IPF Brown angle summary . . . . .	8
2.1	IPF input file begin and end times . . . . .	9
2.2	IPF input file editing status . . . . .	9
2.3	List of Removed Centroids (Original CA File Row Index) . . . . .	11
2.4	List of Removed PCRS Centroids (Original CB File Row Index) . . . . .	11
3.1	Table of figures I (IPF run) . . . . .	12
3.2	Table of figures II (IPF run) . . . . .	13
3.3	PCRS measurement prediction error summary . . . . .	26

# 1 IPF EXECUTION SUMMARY

This report summarizes the SIRTF Instrument Pointing Frame (IPF) Kalman Filter execution associated with run file: RN602095. In particular, this Focal Point Survey calibrates the instrument: MIPS\_24um\_center (95), as part of the IOC Fine Survey. The main calibration results from the IPF filter execution have been documented in IF602095 typically stored in the mission archive DOM collection IPF\_IF. This report only summarizes the main aspects of the run, and does not substitute for the full information contained in the IF file.

Section 1 summarizes the filter execution results. The filter configurations are tabulated in Table 1.2 and the mask vector assignments are tabulated in Table 1.3. A total of 33 state parameters are estimated in this run. The overall End-to-End pointing performances are tabulated in Table 1.4. The prediction residuals throughout the estimation processes are tabulated in Table 1.5. Section 3 summarizes resulting plots, a mini summary of the IF IPF output file, and the execution log. Section 4 captures the user comments that are specific to this particular run.

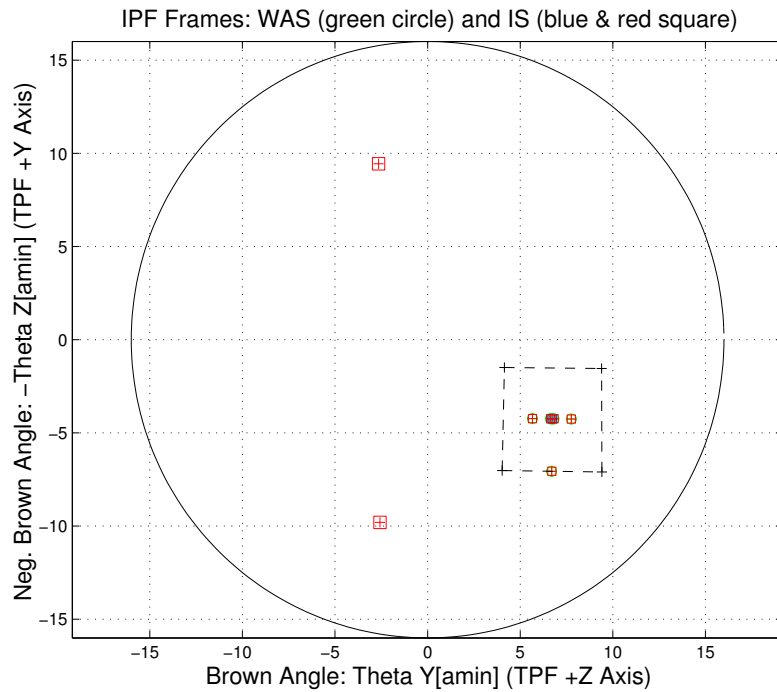


Figure 1.1: A-priori and a-posteriori IPF frames

RAW	FINAL (After Editing)
AA601095	AA601095
AS601095	AS601095
CA601095	CA901095
CB601095	CB601095
CS601095	CS601095

Table 1.1: IPF filter input files

EXECUTION CONFIGURATION ITEM	CURRENT STATUS
IPF Filter Version Used	IPF.V3.0.0B
Frame Table Version Used	BodyFrames_FTU_14a
Scan-Mirror Employed?	YES
IPF Filter Mode	NORMAL-MODE(0)
SLIT-MODE Operation	DISABLED
Kalman Filter Operation	ENABLED
Least-Squares Data Analysis	ENABLED
IBAD Screening	ENABLED
User-Specified Data Editing	DISABLED
Total Number of Iterations	25
LS Residual Sigma Scale	9.45293165E-001
Total Number of Maneuvers	15

Table 1.2: IPF filter execution configuration

Con. Plate Scale			$\Gamma$ Dependent				$\Gamma^2$ Dependent				Linear Plate Scale						Mirror			
$a_{00}$	$b_{00}$	$c_{00}$	$a_{10}$	$b_{10}$	$c_{10}$	$d_{10}$	$a_{20}$	$b_{20}$	$c_{20}$	$d_{20}$	$a_{01}$	$b_{01}$	$c_{01}$	$d_{01}$	$e_{01}$	$f_{01}$	$\alpha$	$\beta$		
1	2	3	4	5	6	7	8	9	10	11	12	13	14	15	16	17	18	19		
1	1	1	1	1	1	1	0	0	0	0	1	1	1	1	1	1	1	1		
IPF (T)			Alignment R						Gyro Drift Bias											
$\theta_1$	$\theta_2$	$\theta_3$	$a_{rx}$	$a_{ry}$	$a_{rz}$	$b_{rx}$	$b_{ry}$	$b_{rz}$	$c_{rx}$	$c_{ry}$	$c_{rz}$	$b_{gx}$	$b_{gy}$	$b_{gz}$	$c_{gx}$	$c_{gy}$	$c_{gz}$			
20	21	22	23	24	25	26	27	28	29	30	31	32	33	34	35	36	37			
1	1	1	1	1	1	1	1	1	1	1	1	1	1	1	1	1	1			

Table 1.3: IPF filter execution mask vector assignment

## FOCAL PLANE SURVEY ANALYSIS: IOC Fine Survey.

INSTRUMENT NAME: MIPS\_24um\_center NF: 95

PIX2RADW: 1.20874169E-005 [rad/pixel] = 2.4932E+000 [arcsec/pixel]

PIX2RADV: 1.25959084E-005 [rad/pixel] = 2.5981E+000 [arcsec/pixel]

FRAME	DESCRIPTION	IPF <sup>1</sup>	SF <sup>2</sup>	TOTAL	REQ
095(P)	MIPS_24um_center	0.0224	0.0855	0.0884	0.14
096(I)	MIPS_24um_plusY_edge	0.0328	0.0855	0.0916	N/A
099(I)	MIPS_24um_small_FOV1	0.0214	0.0855	0.0881	N/A
100(I)	MIPS_24um_small_FOV2	0.0214	0.0855	0.0881	N/A
103(I)	MIPS_24um_large_FOV1	0.0224	0.0855	0.0884	N/A
104(I)	MIPS_24um_large_FOV2	0.0224	0.0855	0.0884	N/A

Table 1.4: IPF calibration error summary ([arcsec], 1-sigma, radial)

RMS METRIC	A PRIORI <sup>3</sup>	A POSTERIORI <sup>3</sup>	ATT. CORRECTED <sup>4</sup>	UNITS
Radial	2.4059	0.1785	0.1634	arcsec
W-Axis	1.4388	0.1059	0.0892	arcsec
V-Axis	1.9283	0.1437	0.1369	arcsec
Radial	0.9401	0.0697	0.0637	pixels
W-Axis	0.5771	0.0425	0.0358	pixels
V-Axis	0.7422	0.0553	0.0527	pixels

Table 1.5: Science measurement prediction error summary (1-sigma)

---

<sup>1</sup>IPF filter removes systematic pointing errors due to: thermomechanical alignment drift (Body to TPF), gyro bias and bias drift, centroiding error, attitude error, and optical distortion. IPF SIGMA presented here is “Scaled” by the Least Squares Scale factor. The Least Squares Scale Factor was: 0.945293. It is assumed that the gyro Angle Random Walk contribution is captured with the Least Squares scaling. The gyro ARW contribution can be approximately calculated as 0.0517 arcseconds, given that ARW = 100  $\mu\text{deg}/\sqrt{\text{hr}}$ , with 5.567000e+002 second Maneuver time (max), and 15 independent Maneuvres.

<sup>2</sup>Gyro Scale Factor(GSF) assumes 95 ppm error over 0.250 degree maneuver.

<sup>3</sup>This can be interpreted as estimate of ”pixel to sky” pointing reconstruction error if no science data is used.

<sup>4</sup>This can be interpreted as estimate of achieved S/I centroiding error

IPF BROWN ANGLE SUMMARY					
FRAME TABLE USED: BodyFrames_FTU_14a					
NF	NAME	WAS	IS	CHANGE	UNIT
095	theta_Y	+6.716105	+6.721826	+0.005721	arcmin
095	theta_Z	+4.246060	+4.243820	-0.002240	arcmin
095	angle	+0.637930	+0.628212	-0.009717	deg
096	theta_Y	+6.695190	+6.703859	+0.008670	arcmin
096	theta_Z	+7.060913	+7.055562	-0.005350	arcmin
096	angle	+0.637930	+0.628212	-0.009717	deg
099	theta_Y	+7.756798	+7.762937	+0.006139	arcmin
099	theta_Z	+4.259313	+4.257169	-0.002144	arcmin
099	angle	+0.637930	+0.628212	-0.009717	deg
100	theta_Y	+5.659609	+5.665074	+0.005465	arcmin
100	theta_Z	+4.234140	+4.231696	-0.002444	arcmin
100	angle	+0.637930	+0.628212	-0.009717	deg
103	theta_Y	+6.819955	+6.825711	+0.005755	arcmin
103	theta_Z	+4.247316	+4.245090	-0.002225	arcmin
103	angle	+0.637930	+0.628212	-0.009717	deg
104	theta_Y	+6.633060	+6.638755	+0.005695	arcmin
104	theta_Z	+4.245067	+4.242815	-0.002252	arcmin
104	angle	+0.637930	+0.628212	-0.009717	deg

Table 1.6: IPF Brown angle summary

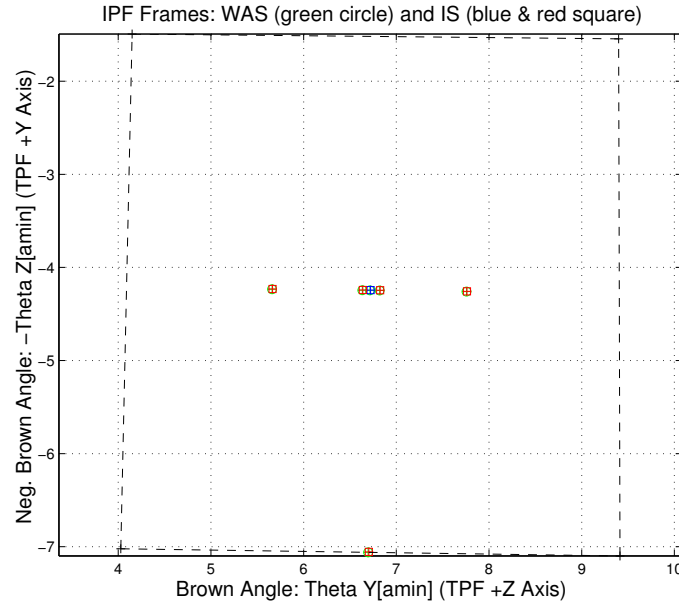


Figure 1.2: A-priori and a-posteriori IPF frames (ZOOMED)

## 2 IPF INPUT FILE HISTORY

STATUS	FILENAME	START TIME	END TIME
WAS	AA601095	753575500.4	753587499.3
IS	AA601095	753575500.4	753587499.3
WAS	CA601095	753576046.5	753586613.5
IS	CA901095	753576046.5	753586613.5
WAS	CB601095	753575861.9	753586745.4
IS	CB601095	753575861.9	753586745.4

Table 2.1: IPF input file begin and end times

WAS	SIZE	IS	SIZE	REMOVED	PATCHED
AA601095	119990	AA601095	119990	0	0
CA601095	467	CA901095	460	7	N/A
CB601095	126	CB601095	126	0	N/A

Table 2.2: IPF input file editing status

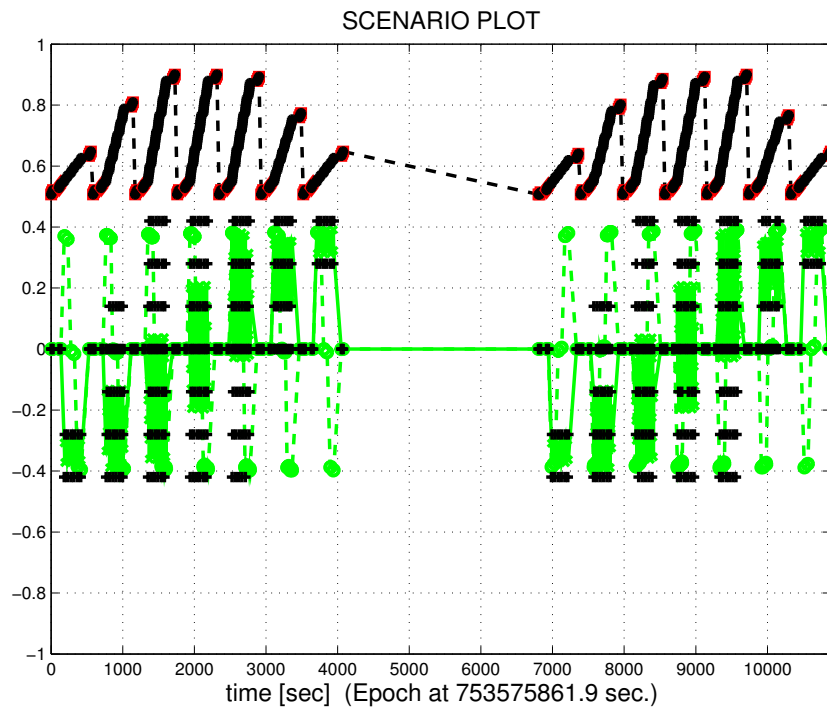


Figure 2.1: Scenario Plot

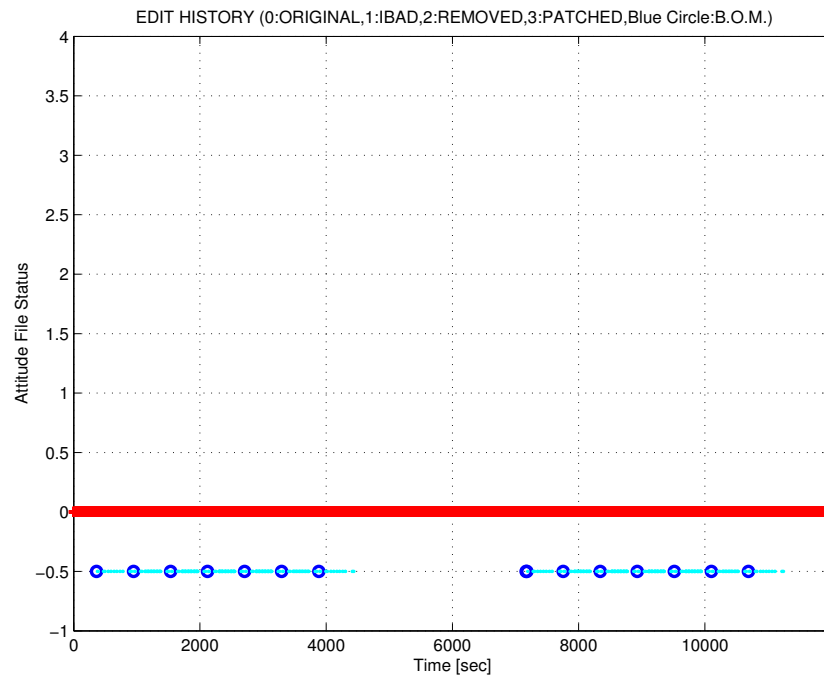


Figure 2.2: Attitude file edit history

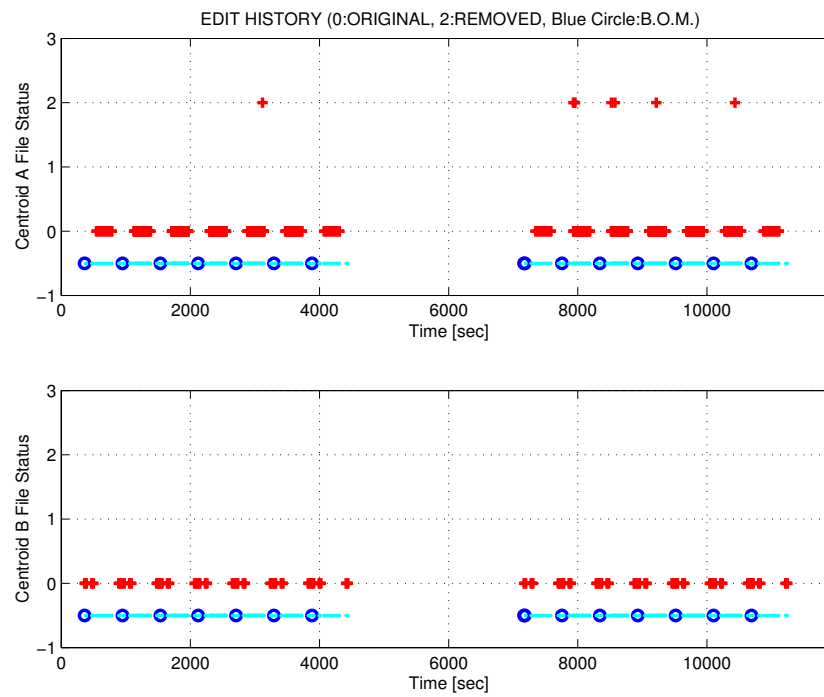


Figure 2.3: Centroid file edit history

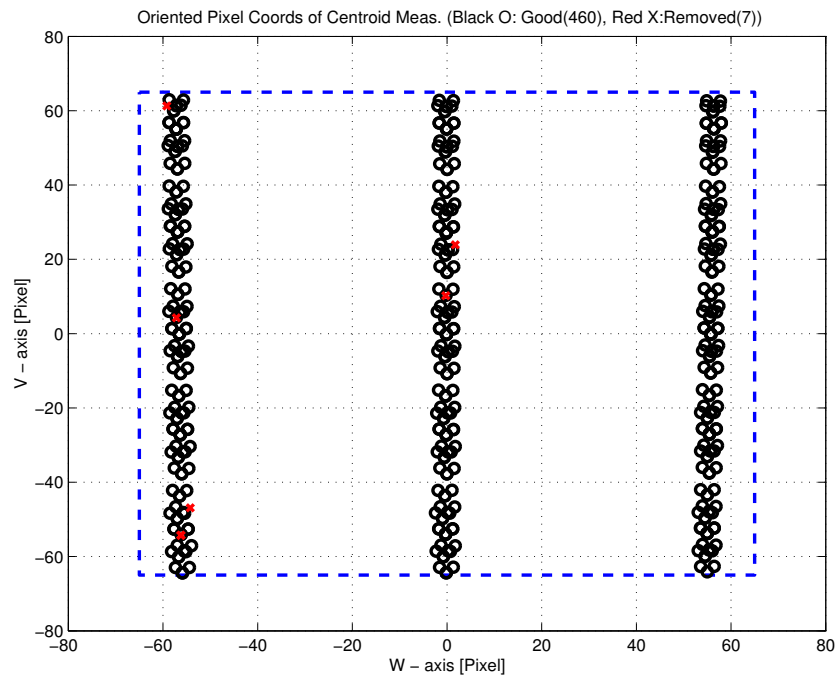


Figure 2.4: Oriented Pixel Coords of Centroid Meas. Edited Centroids

LIST OF REMOVED SCIENCE CENTROIDS						
185	246	251	283	294	351	444

Table 2.3: List of Removed Centroids (Original CA File Row Index)

LIST OF REMOVED PCRS CENTROIDS								

Table 2.4: List of Removed PCRS Centroids (Original CB File Row Index)

### 3 IPF EXECUTION RESULTS

#### 3.1 IPF EXECUTION OUTPUT PLOTS

This subsection summarizes the IPF filter results. As shown in Table 3.1, the output plots are segmented to three groups: predicted performance, post-run results and IPF trending plots.

FIGURE NO.	DESCRIPTION
<b>Predicted performance prior to IPF run</b>	
Figure 3.1	Meas. and a-priori predicts in TPF coords
Figure 3.2	Meas. and a-priori predicts in Oriented Pixel Coords including rectangular array boundary approximation
Figure 3.3	A-Priori Prediction Error Quiver Plot in Oriented Pixel Coords including rectangular array boundary approximation
Figure 3.4	A-priori prediction error
Figure 3.5	Oriented Pixel Coords of measurements and a-priori predicts (PCRS only)
Figure 3.6	Oriented Pixel Coords of measurements and a-priori predicts (Zoomed, PCRS only)
Figure 3.7	Oriented (W,V) Pixel Coords of A-Priori PCRS Prediction Error Quiver Plot
Figure 3.8	A-priori PCRS prediction error
<b>IPF filter performance (post run results)</b>	
Figure 3.9	IPF execution convergence, chart 1: (top) normalized residual error vs. iteration number and (bottom) norm of effective parameter corrections
Figure 3.10	IPF execution convergence, chart 2: parameter correction size vs. iteration number
Figure 3.11	Parameter uncertainty convergence: square-root of diagonal elements of covariance matrix vs. maneuver number
Figure 3.12	IPF parameter symbol table
Figure 3.13	KF parameter error sigma plot (a-priori-dashed, a-posteriori-solid). Includes true parameter errors (FLUTE runs only)
Figure 3.14	LS parameter error sigma plot. Includes true parameter errors (FLUTE runs only)
Figure 3.15	KF and LS parameter errors sigma plot (Figure 3.13 & Figure 3.14 combined)
Figure 3.16	Measurements and a-posteriori predicts in Oriented Pixel Coords including rectangular array boundaries (a-priori-dashed, a-posteriori-solid)
Figure 3.17	Attitude corrected meas. and a-posteriori predicts in Oriented Pixel Coords including rectangular array boundaries (a-priori-dashed, a-posteriori-solid)

Table 3.1: Table of figures I (IPF run)

FIGURE NO.	DESCRIPTION
<b>IPF filter performance (post run results) - CONTINUE</b>	
Figure 3.18	KF innovations with (o) and w/o (+) attitude corrections
Figure 3.19	Histograms of science a-posteriori residuals (or innovations)
Figure 3.20	A-Posteriori Science Centroid Prediction Error Quiver (Att. Cor.)
Figure 3.21	Normalized A-Posteriori Science Centroid Prediction Errors
Figure 3.22	KF innovations with (o) and w/o (+) attitude corrections (PCRS)
Figure 3.23	Histograms of PCRS a-posteriori residuals (or innovations)
Figure 3.24	A-posteriori PCRS Prediction Summary
Figure 3.25	A-posteriori PCRS Prediction (PCRS 1 Only)
Figure 3.26	A-posteriori PCRS Prediction (PCRS 2 Only)
Figure 3.27	A-Posteriori PCRS Prediction Errors Quiver (Att. Cor.)
Figure 3.28	Normalized A-Posteriori PCRS Prediction Errors
Figure 3.29	W-axis KF innovations and 1-sigma bound
Figure 3.30	V-axis KF innovations and 1-sigma bound
Figure 3.31	Array plot with (solid) and w/o (dashed) optical distortion corrections
Figure 3.32	Optical Distortion Plot: total (x5 magnification)
Figure 3.33	Optical Distortion Plot: constant plate scales (x5 magnification)
Figure 3.34	Optical Distortion Plot: linear plate scale (x5 magnification)
Figure 3.35	Optical Distortion Plot: gamma terms (x5 magnification)
Figure 3.36	Scan Mirror Chops
Figure 3.37	IPF Frame Reconstruction
Figure 3.38	Center Pixel Reconstruction
<b>IPF parameter trending plots</b>	
Figure 3.39	Estimated attitude corrections (Body frame)
Figure 3.40	Estimated attitude error sigma plot (Body frame)
Figure 3.41	Systematic error attributed to thermo-mechanical boresight drift (equiv. angle in (W,V) coords)
Figure 3.42	Systematic error attributed to thermo-mechanical boresight drift (equiv. angle in Body frame)
Figure 3.43	Systematic error attributed to gyro drift bias (equiv. rate in (W,V) coords)
Figure 3.44	Systematic error attributed to gyro drift bias (equiv. angle in (W,V) coords)
Figure 3.45	Systematic error attributed to gyro drift bias (equiv. angle in Body frame)

Table 3.2: Table of figures II (IPF run)

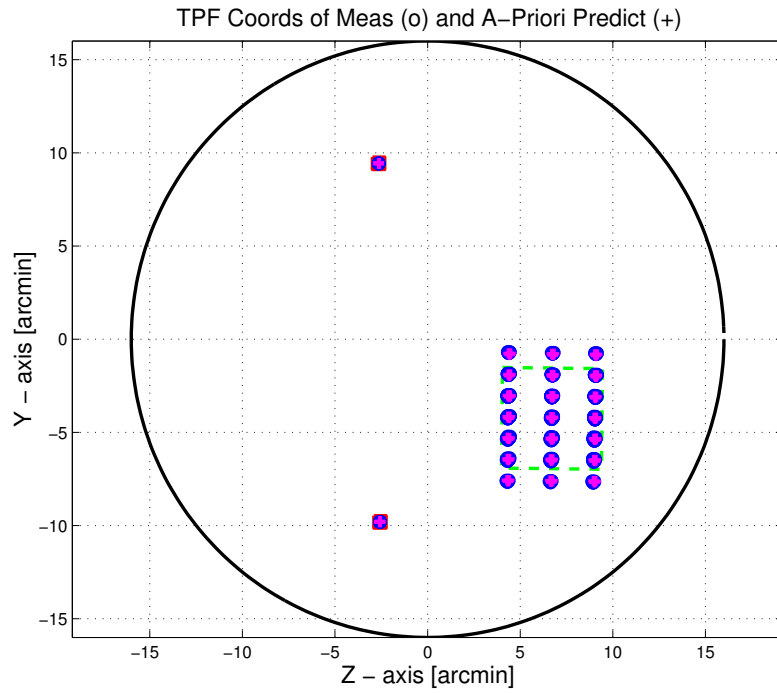


Figure 3.1: TPF coords of measurements and a-priori predicts

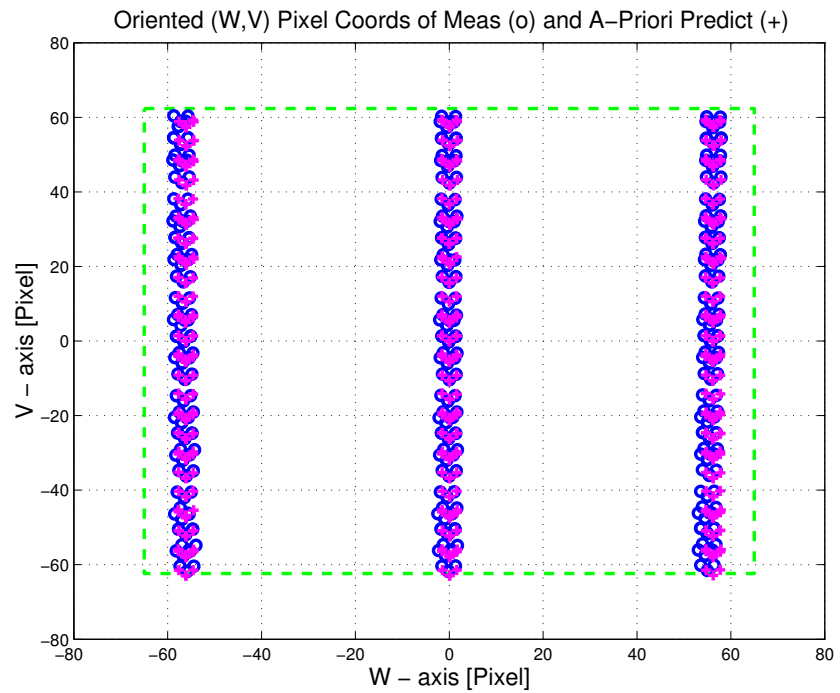


Figure 3.2: Oriented PixelCoords of measurements and a-priori predicts

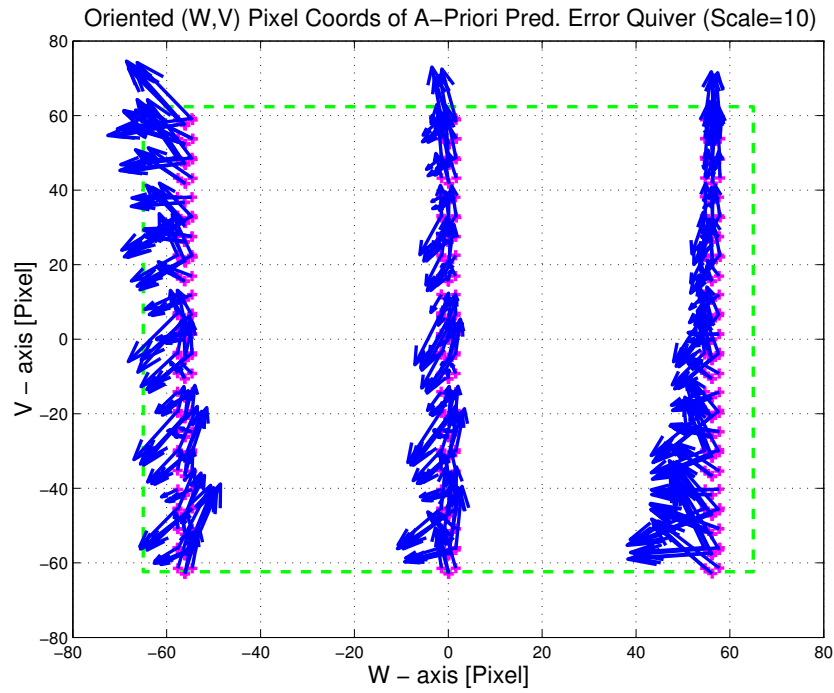


Figure 3.3: Oriented (W,V) Pixel Coords of A-Priori Prediction Error Quiver Plot

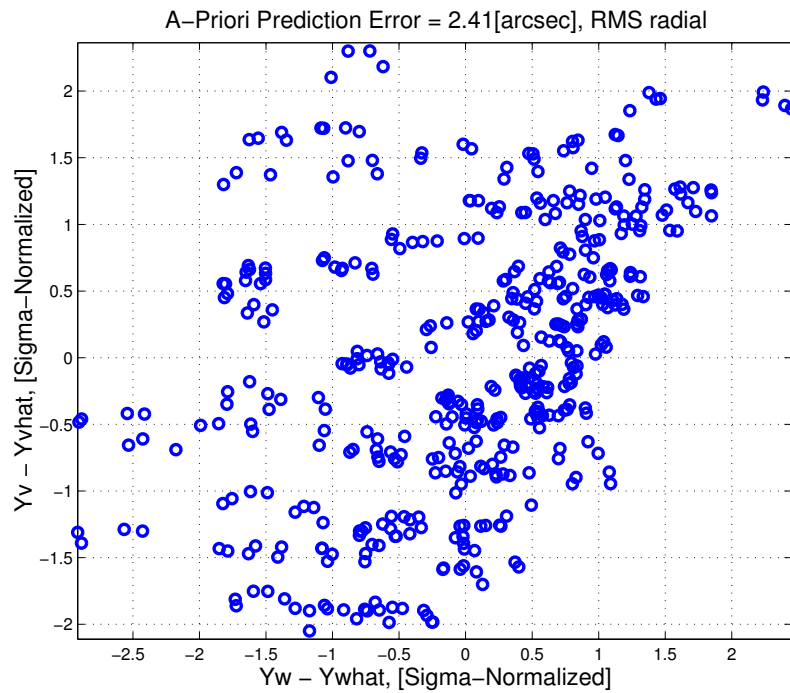


Figure 3.4: A-priori prediction error (Science Centroids)

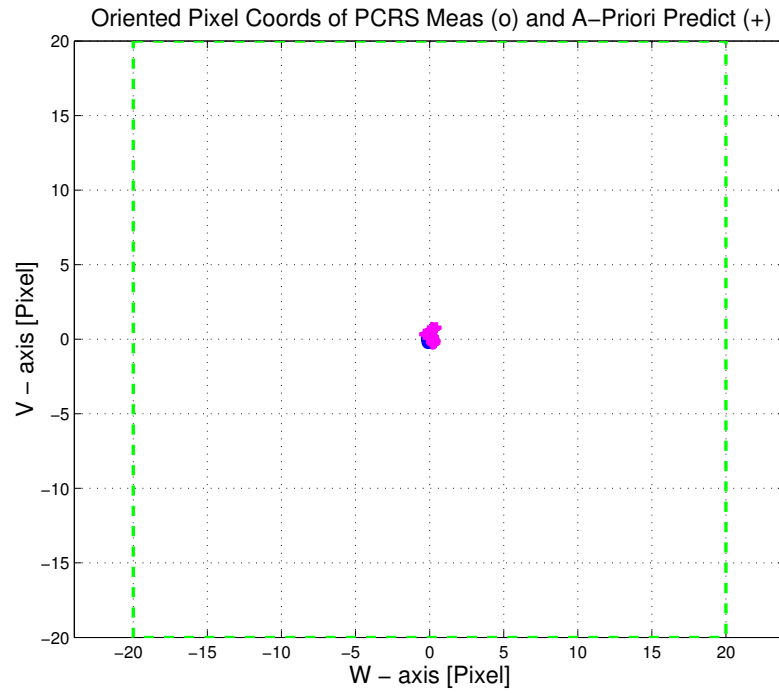


Figure 3.5: Oriented Pixel Coords of measurements and a-priori predicts (PCRS only)

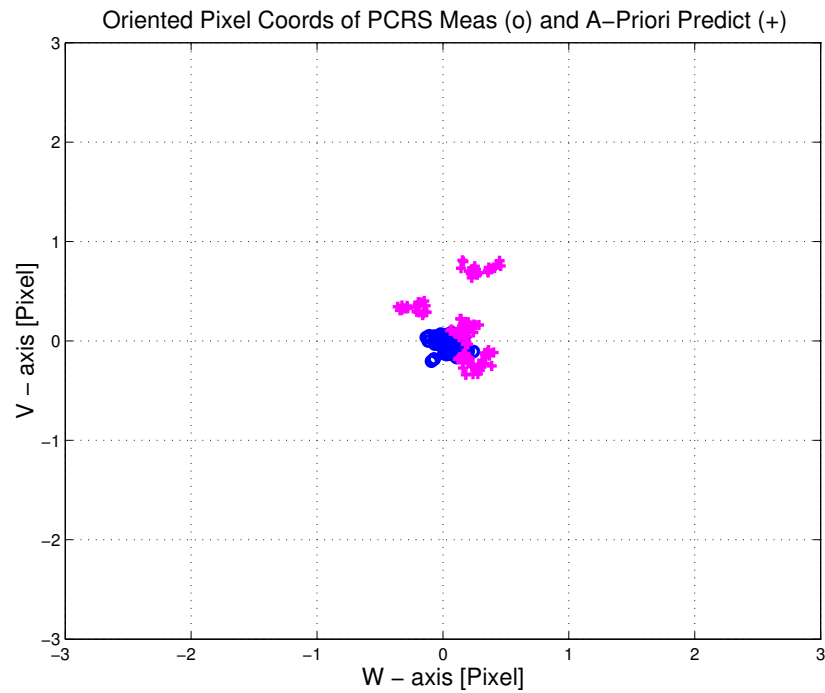


Figure 3.6: Oriented Pixel Coords of measurements and a-priori predicts (Zoomed, PCRS only)

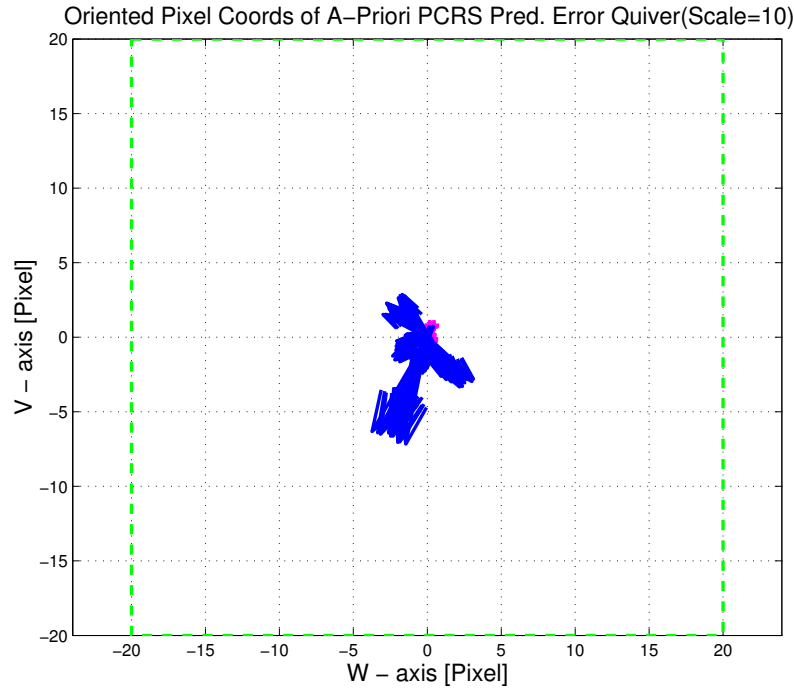


Figure 3.7: Oriented (W,V) Pixel Coords of A-Priori PCRS Prediction Error Quiver Plot

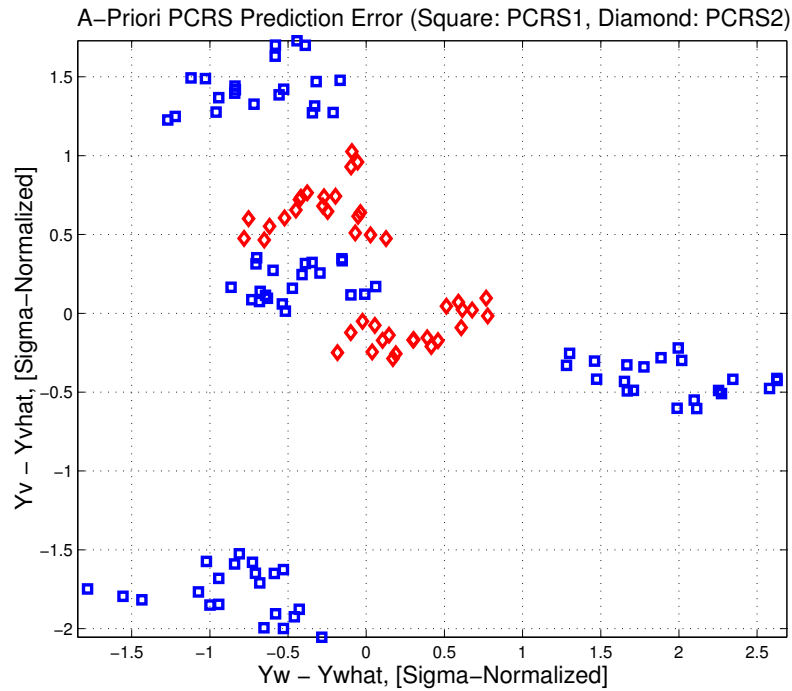


Figure 3.8: A-priori PCRS prediction error

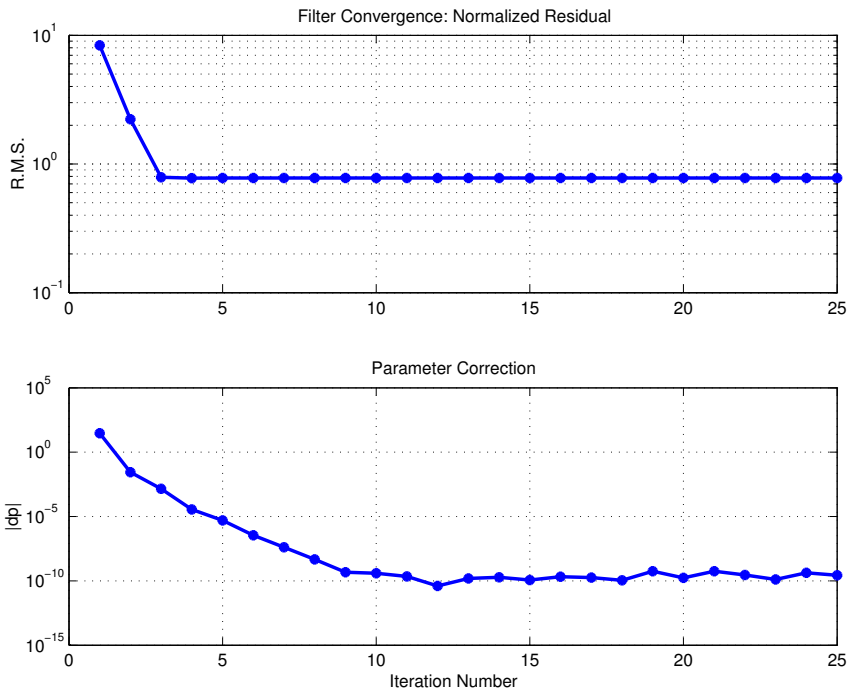


Figure 3.9: IPF execution convergence, chart 1

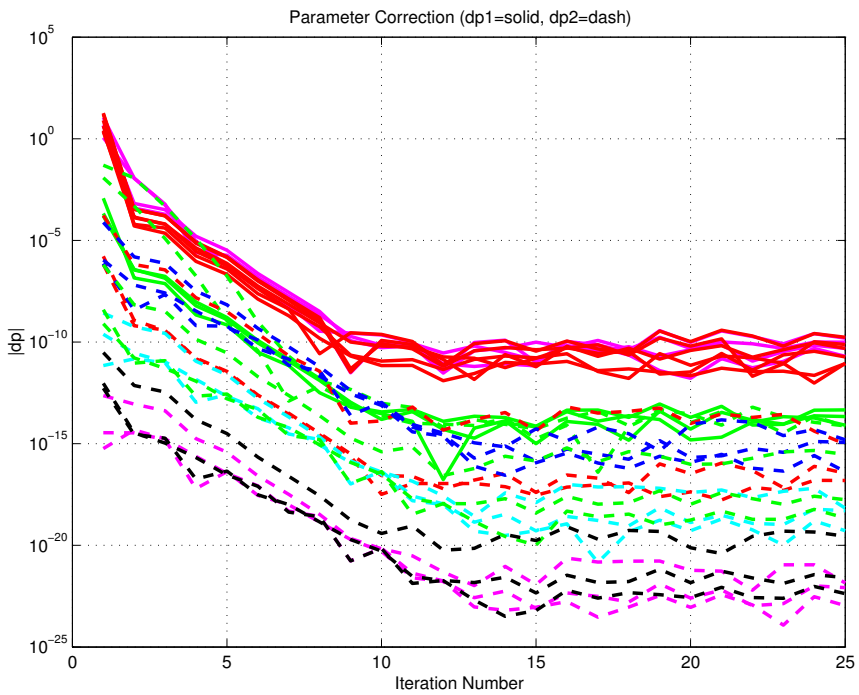


Figure 3.10: IPF execution convergence, chart 2

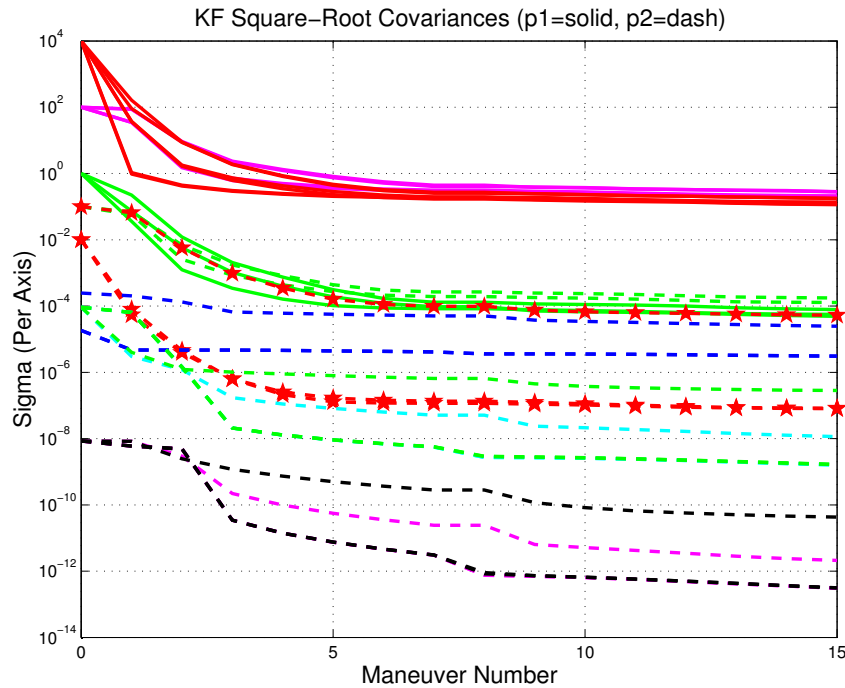


Figure 3.11: Parameter uncertainty convergence

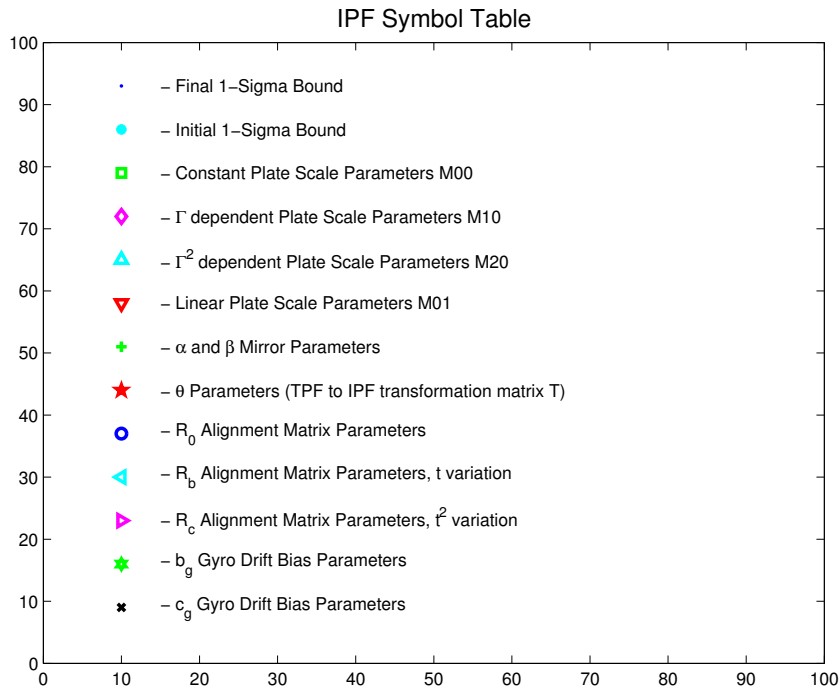


Figure 3.12: IPF parameter symbol table

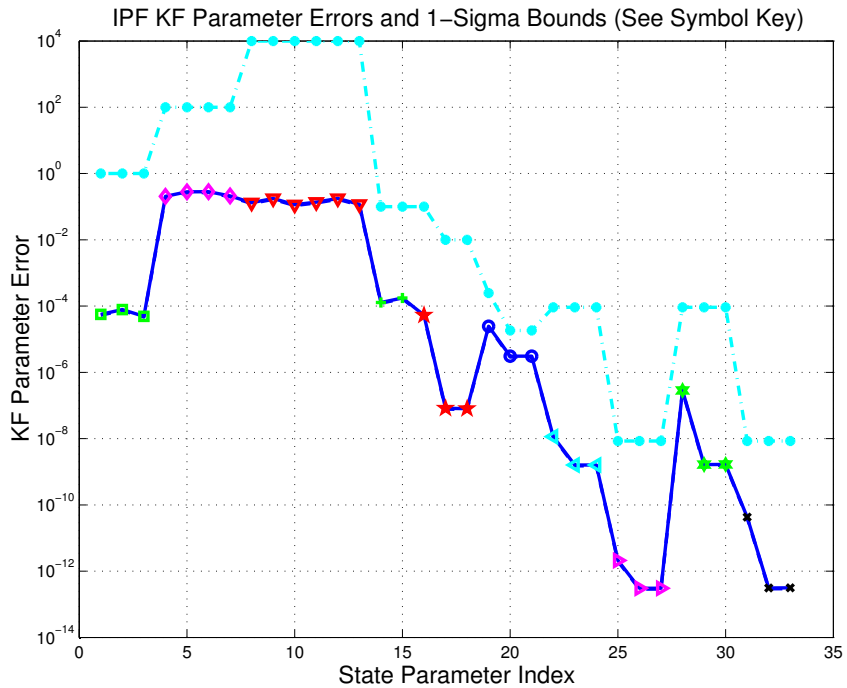


Figure 3.13: KF parameter error sigma plots

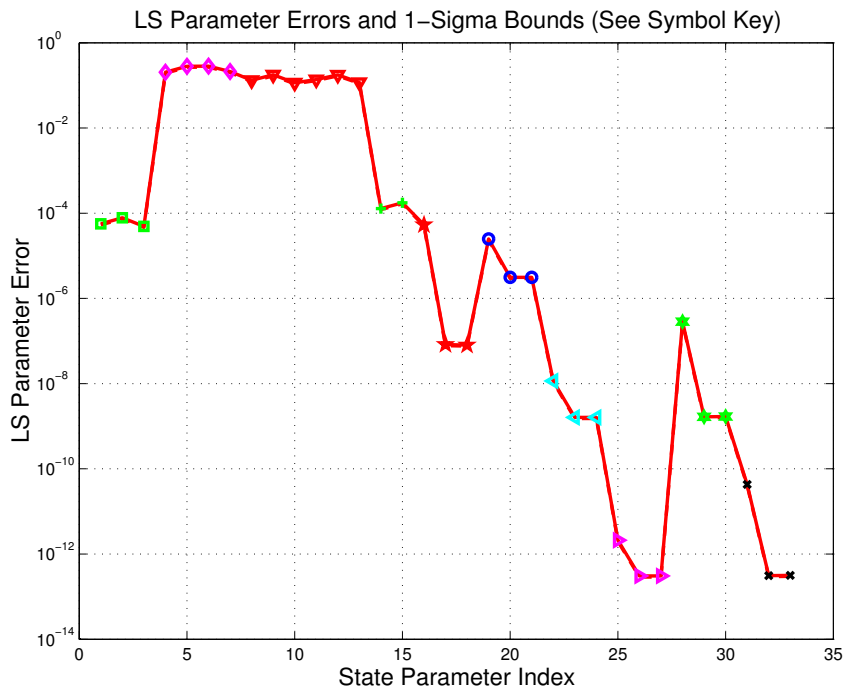


Figure 3.14: LS parameter error sigma plot

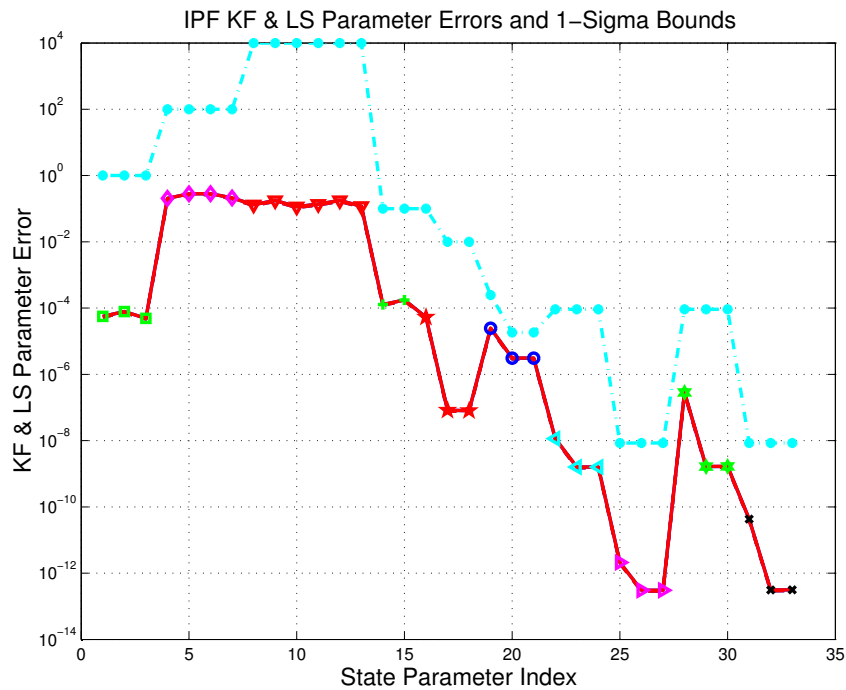


Figure 3.15: KF and LS parameter error sigma plot

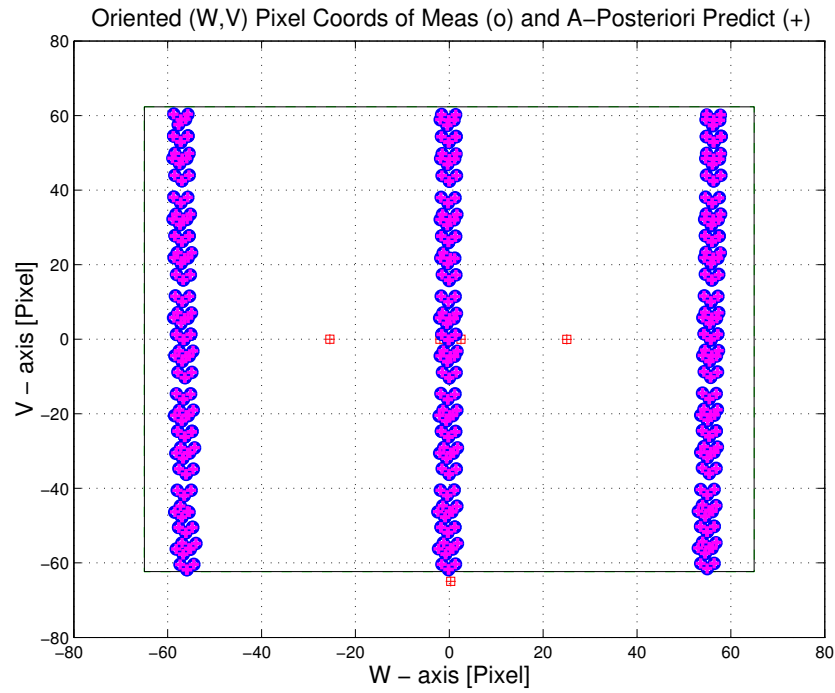


Figure 3.16: Oriented Pixel Coords of meas. and a-posteriori predicts

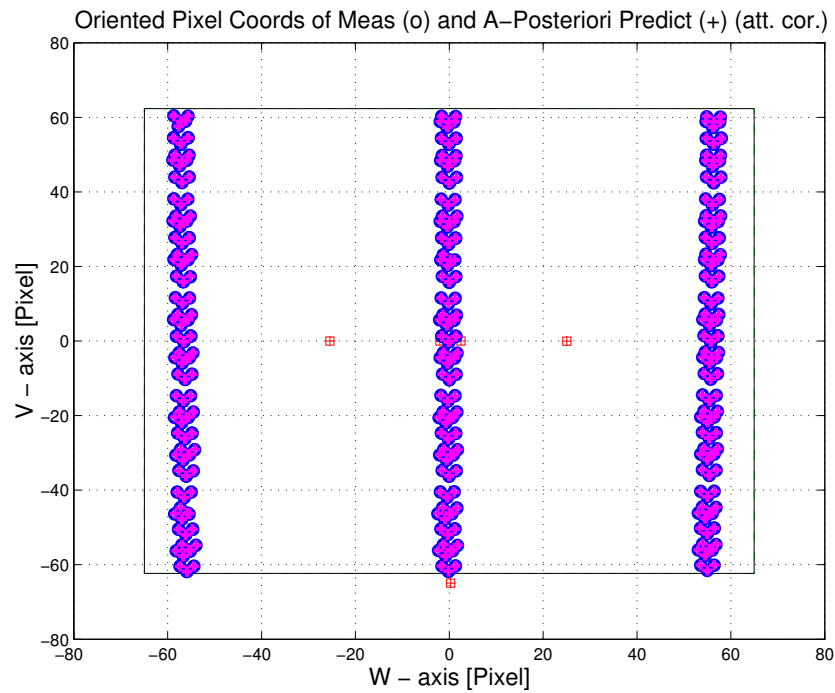


Figure 3.17: Oriented Pixel Coords of meas. and a-posteriori predicts (attitude corrected)

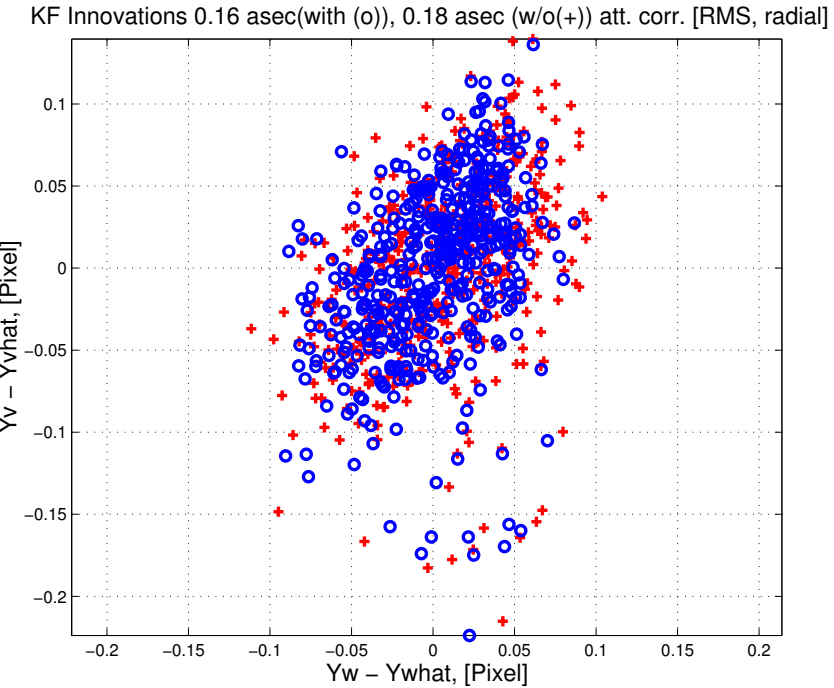


Figure 3.18: KF innovations with (o) and w/o (+) attitude corrections

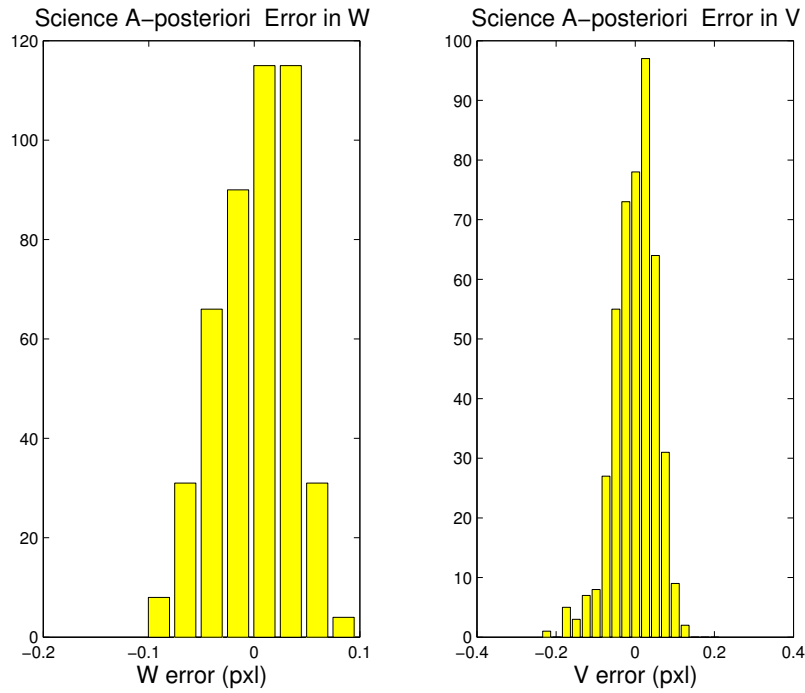


Figure 3.19: Histograms of science a-posteriori residuals (or innovations)

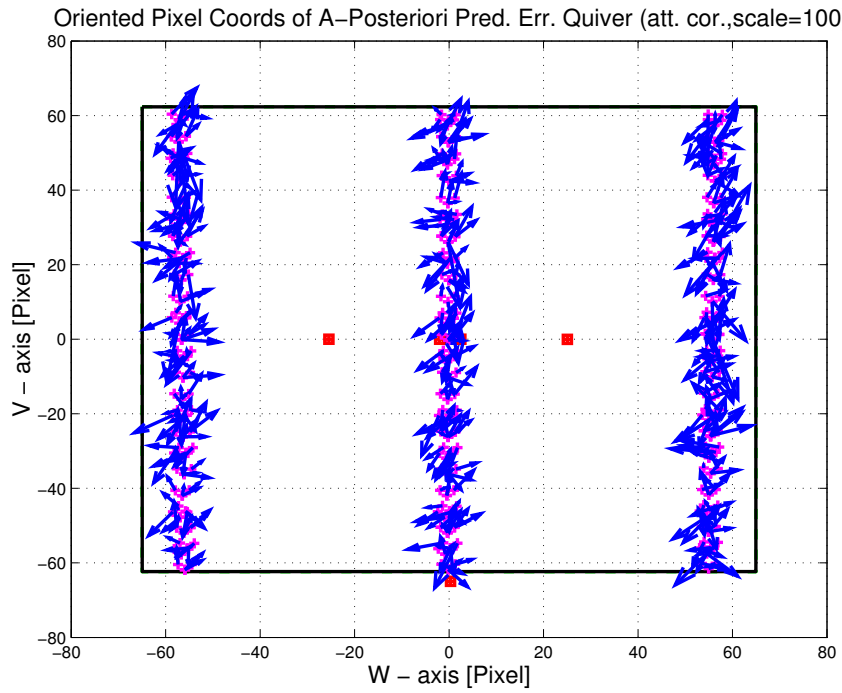


Figure 3.20: A-Posteriori Science Centroid Prediction Error Quiver (Att. Cor.)

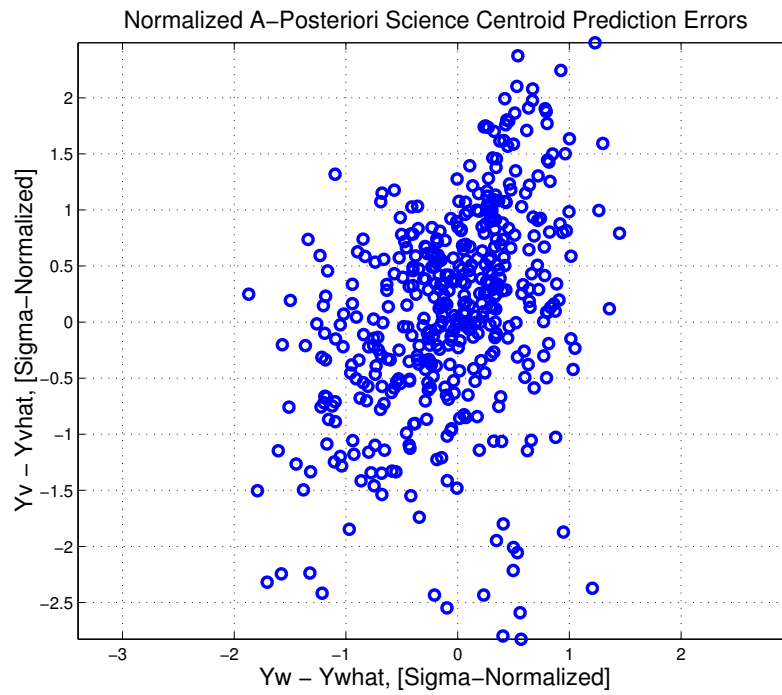


Figure 3.21: Normalized A-Posteriori Science Centroid Prediction Errors

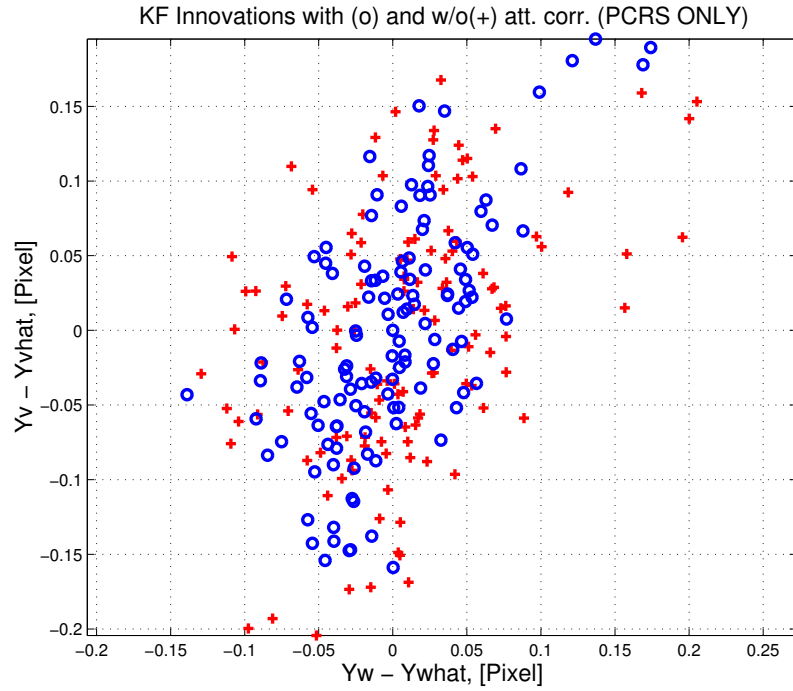


Figure 3.22: KF innovations with (o) and w/o (+) attitude corrections (PCRS)

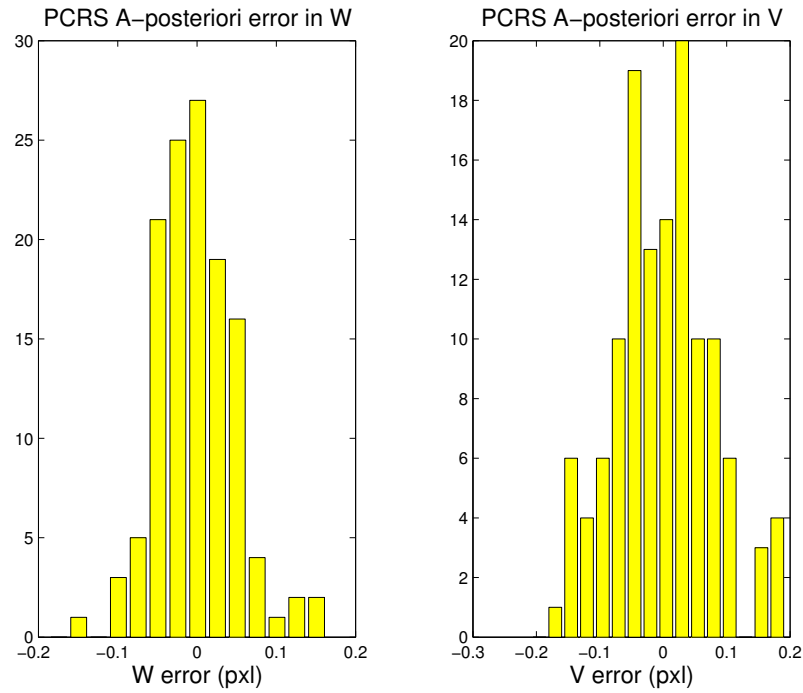


Figure 3.23: Histograms of PCRS a-posteriori residuals (or innovations)

IPF PCRS SUMMARY						
PCRS 1 (Total of 84 centroids)						
RMS	MEAN		SIGMA			
METRIC	APOST.	ATT. COR.	APOST.	ATT. COR.	STAT. CONF.	UNITS
Radial	0.0077	0.0059	0.1144	0.1034	0.0113	arcsec
W-axis	0.0069	-0.0000	0.0705	0.0559	0.0061	arcsec
V-axis	0.0035	0.0059	0.0901	0.0869	0.0095	arcsec
PCRS 2 (Total of 42 centroids)						
METRIC	APOST.	ATT. COR.	APOST.	ATT. COR.	STAT. CONF.	UNITS
Radial	0.0185	0.0132	0.0785	0.0588	0.0091	arcsec
W-axis	0.0076	0.0000	0.0474	0.0346	0.0053	arcsec
V-axis	-0.0168	-0.0132	0.0625	0.0475	0.0073	arcsec
Combined (Total of 126 centroids)						
METRIC	APOST.	ATT. COR.	APOST.	ATT. COR.	STAT. CONF.	UNITS
Radial	0.0079	0.0005	0.1043	0.0914	0.0081	arcsec
W-axis	0.0071	-0.0000	0.0638	0.0499	0.0044	arcsec
V-axis	-0.0033	-0.0005	0.0825	0.0766	0.0068	arcsec

Table 3.3: PCRS measurement prediction error summary

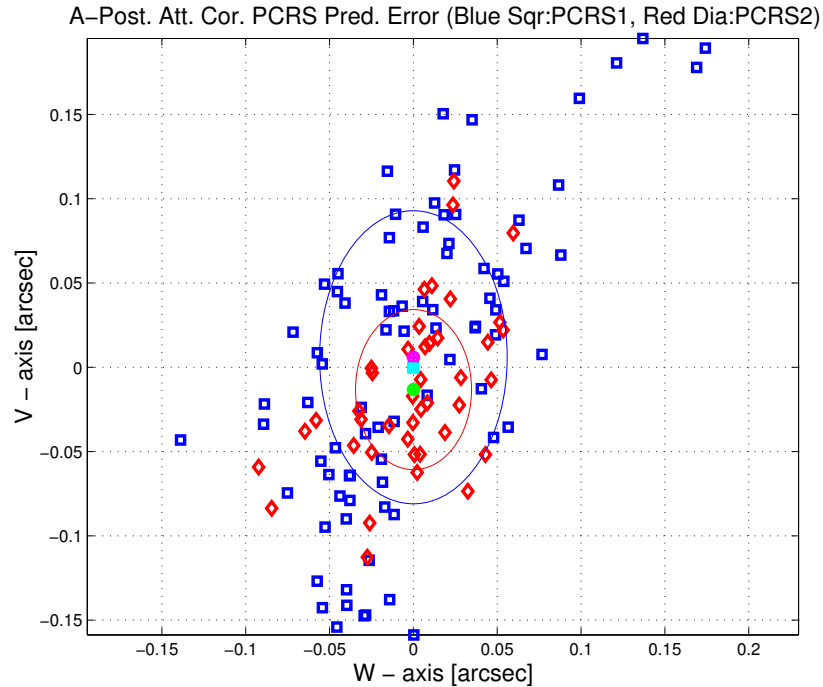


Figure 3.24: A-posteriori PCRS Prediction Summary

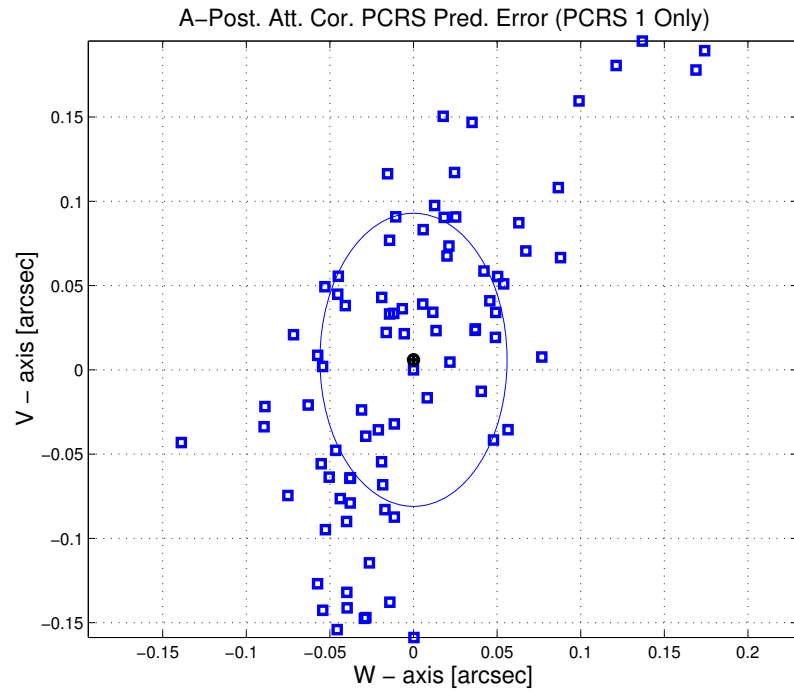


Figure 3.25: A-posteriori PCRS Prediction (PCRS 1 Only)

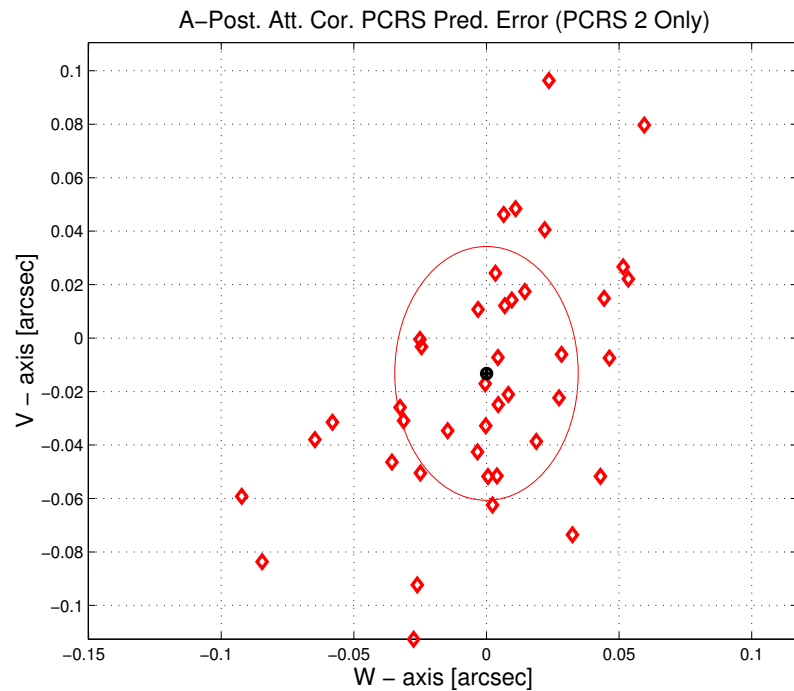


Figure 3.26: A-posteriori PCRS Prediction (PCRS 2 Only)

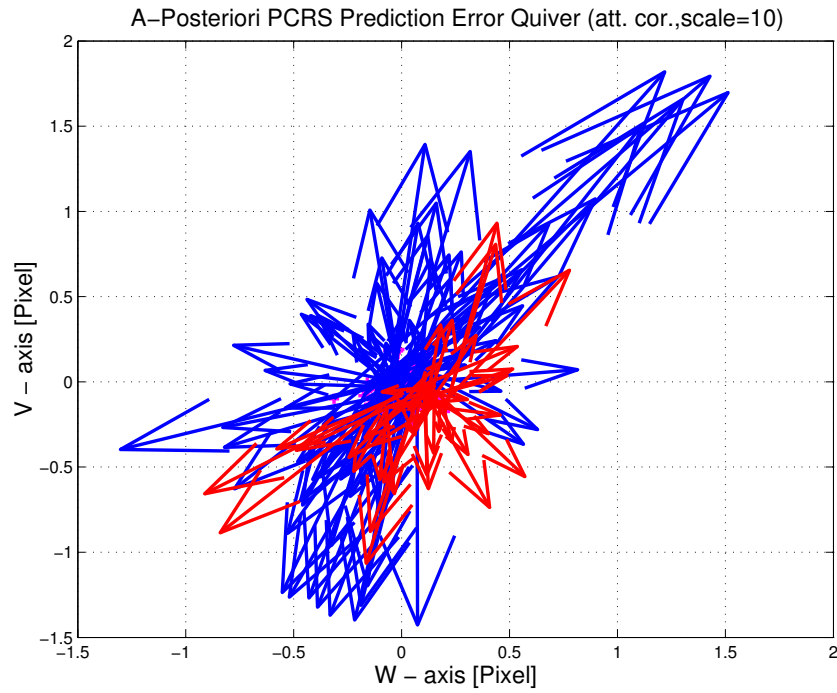


Figure 3.27: A–Posteriori PCRS Prediction Errors Quiver (Att. Cor.)

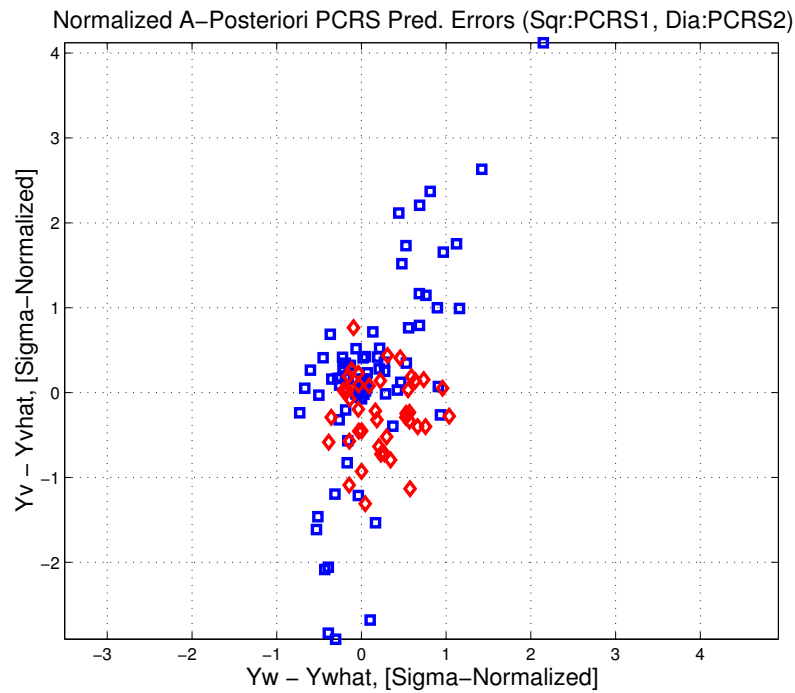


Figure 3.28: Normalized A–Posteriori PCRS Prediction Errors

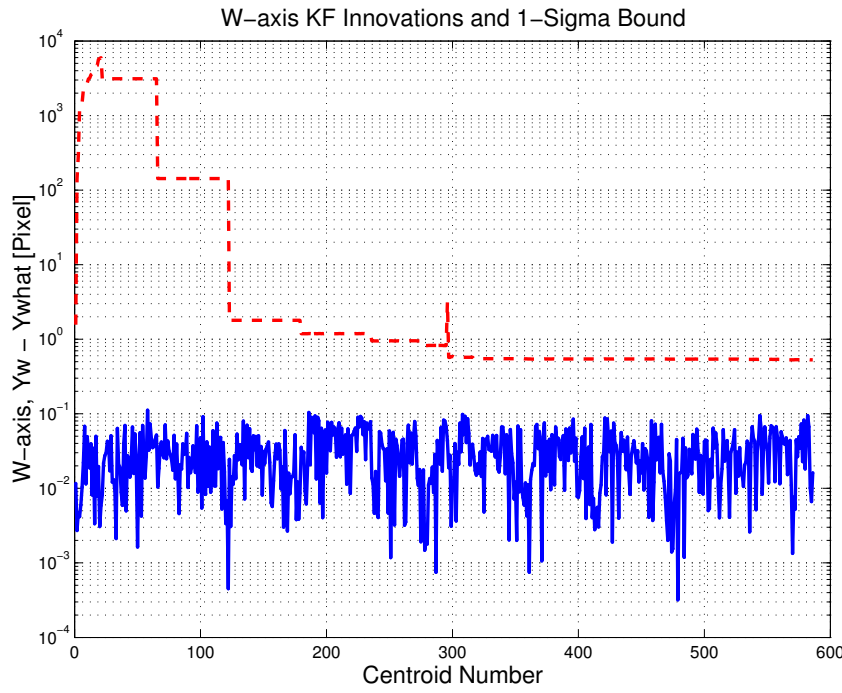


Figure 3.29: W-axis KF innovations and 1-sigma bound

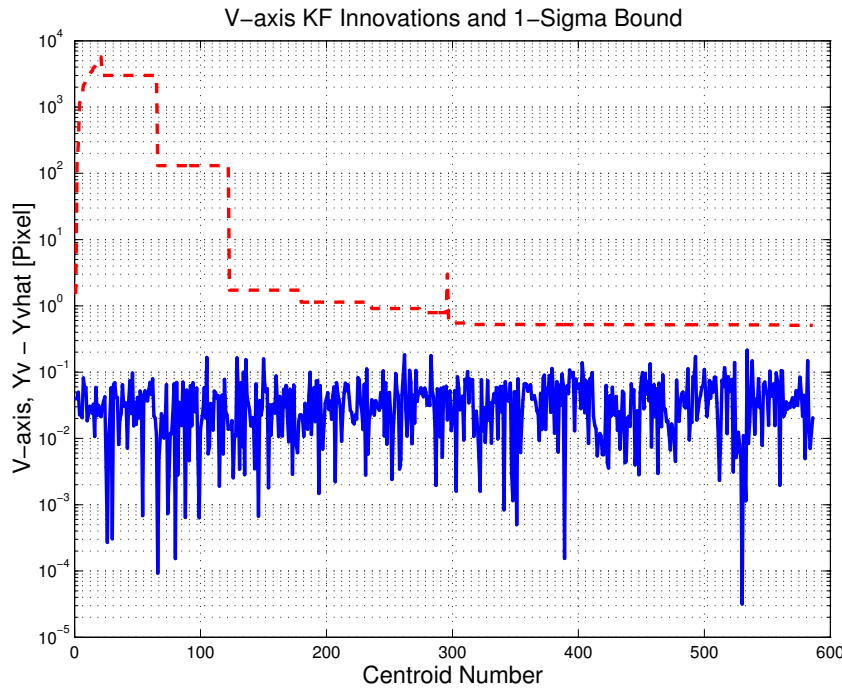


Figure 3.30: V-axis KF innovations and 1-sigma bound

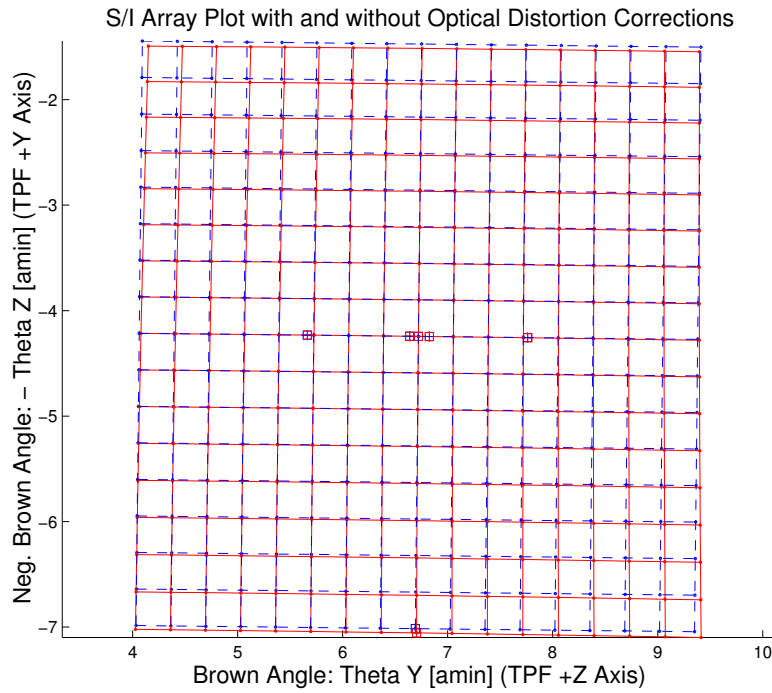


Figure 3.31: Array plot with (solid) and w/o (dashed) optical distortion corrections

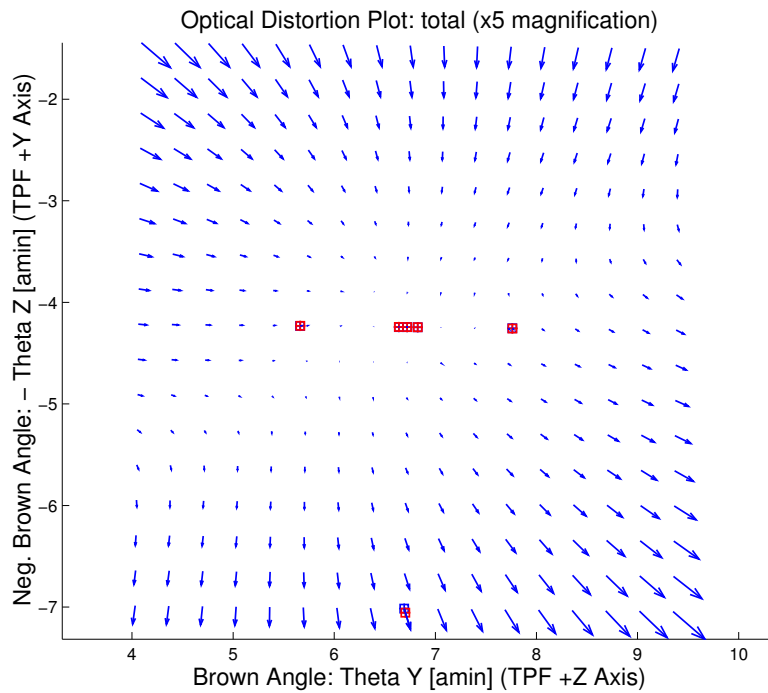


Figure 3.32: Optical Distortion Plot: total (x5 magnification)

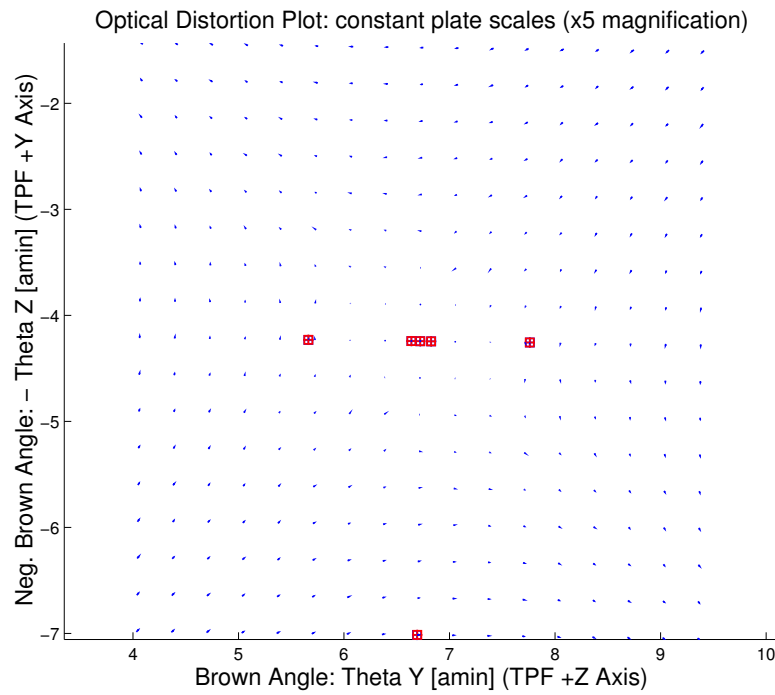


Figure 3.33: Optical Distortion Plot: constant plate scales (x5 magnification)

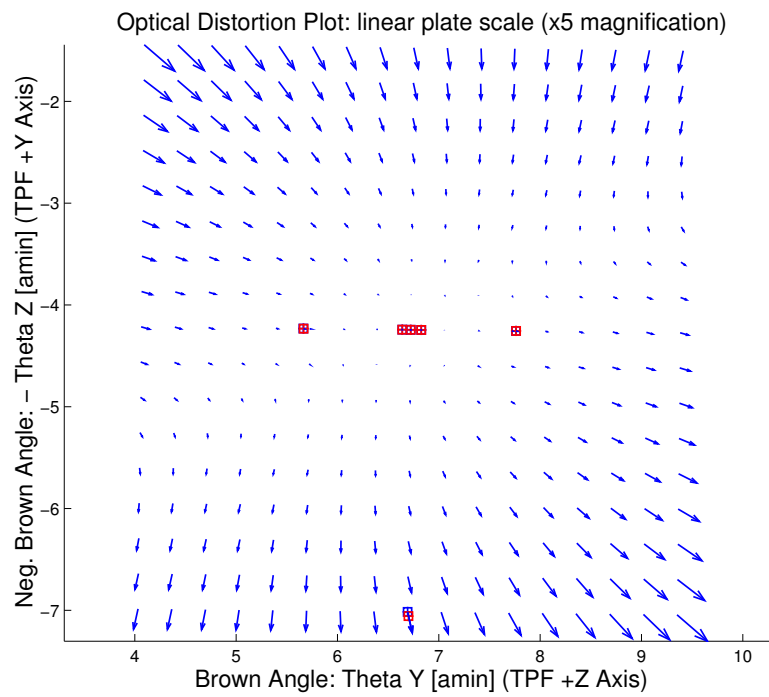


Figure 3.34: Optical Distortion Plot: linear plate scale (x5 magnification)

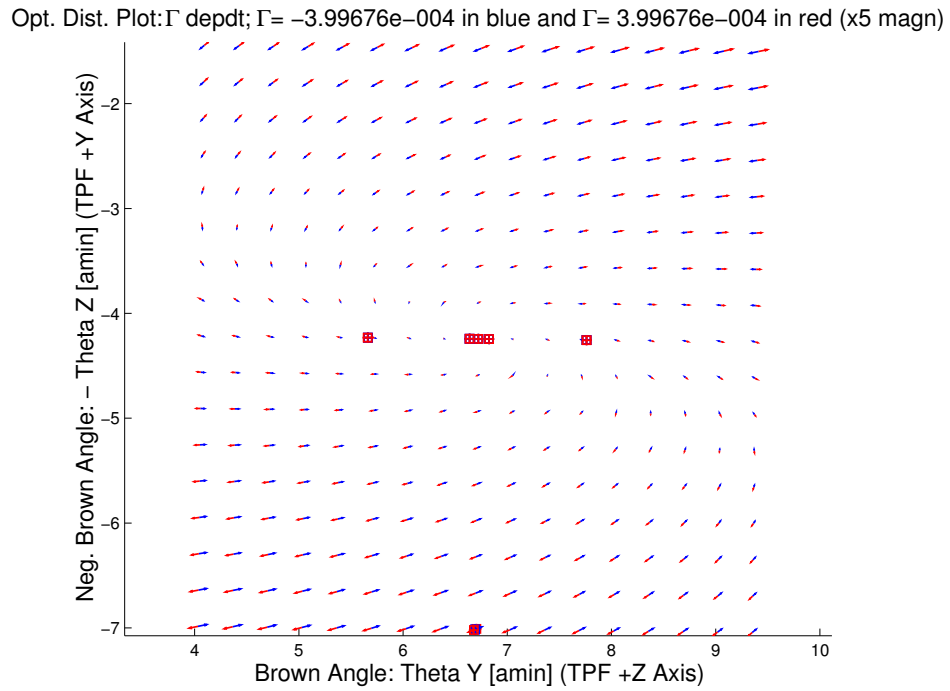


Figure 3.35: Optical Distortion Plot: gamma terms (x5 magnification)

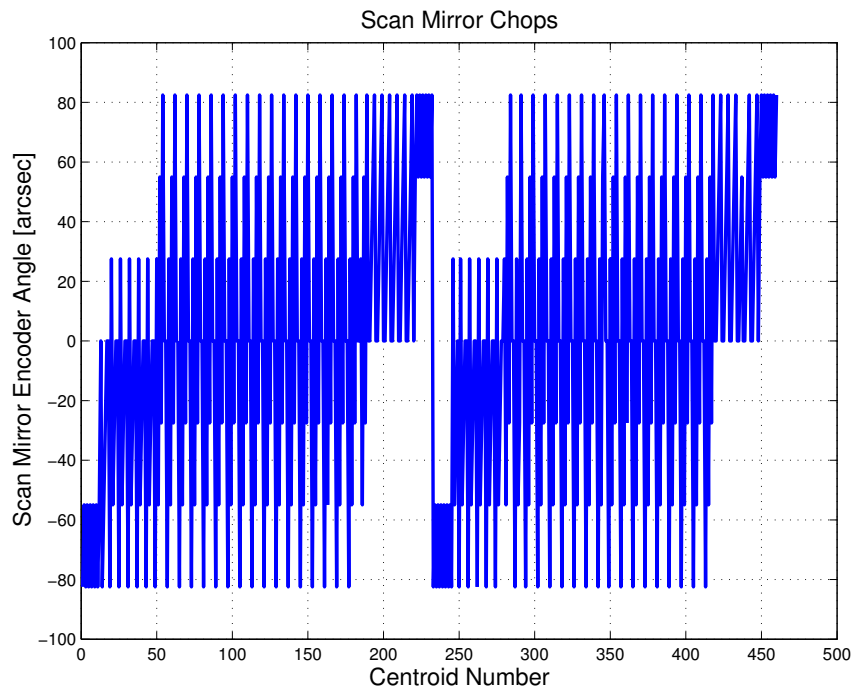


Figure 3.36: Scan Mirror Chops

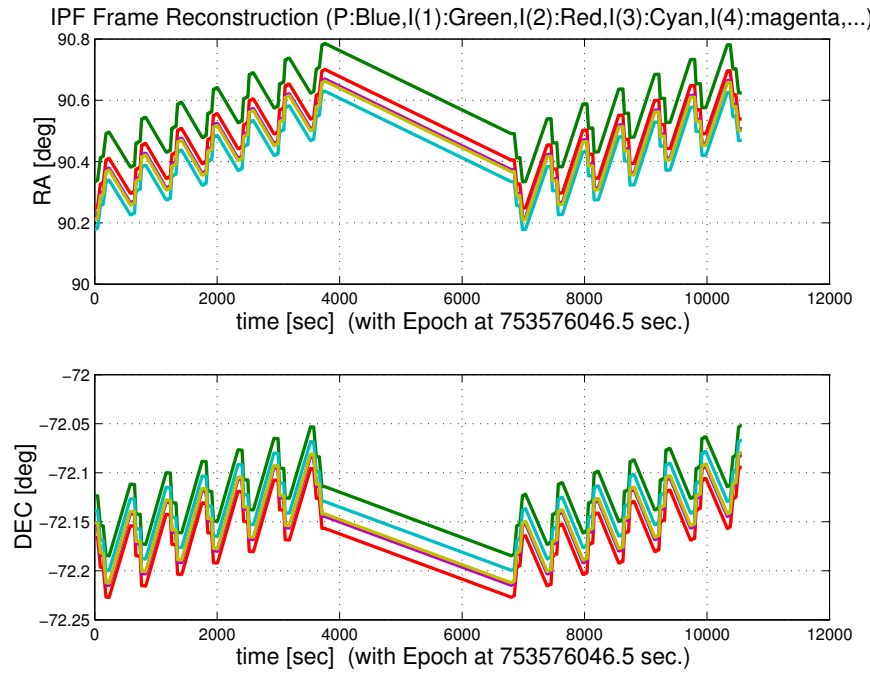


Figure 3.37: IPF Frame Reconstruction

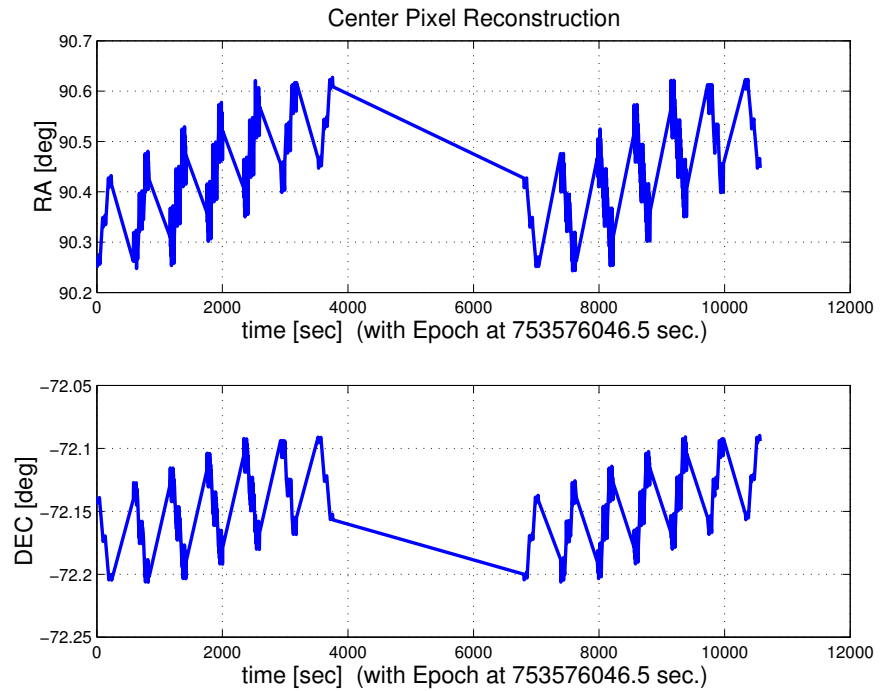


Figure 3.38: Center Pixel Reconstruction

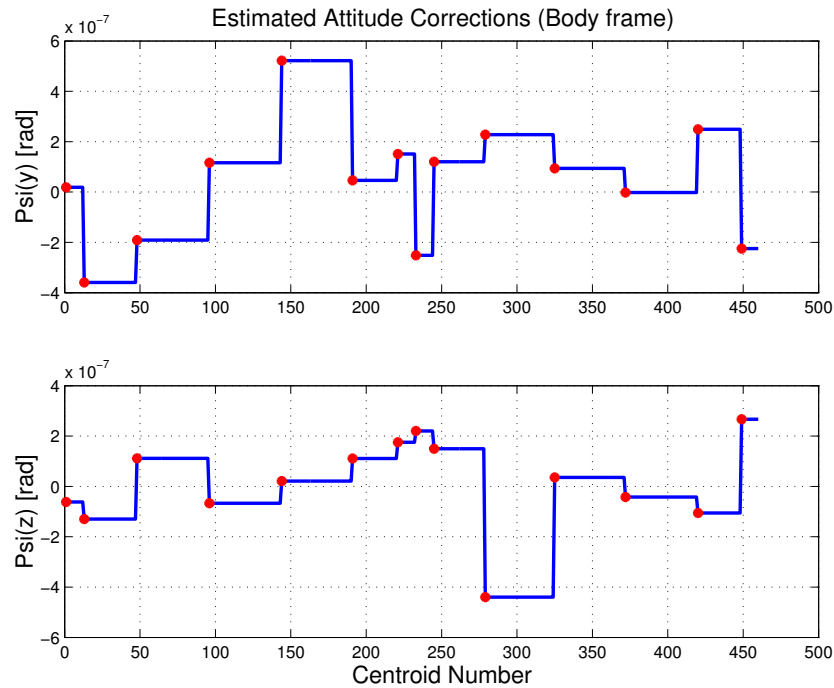


Figure 3.39: Estimated attitude corrections (Body frame)

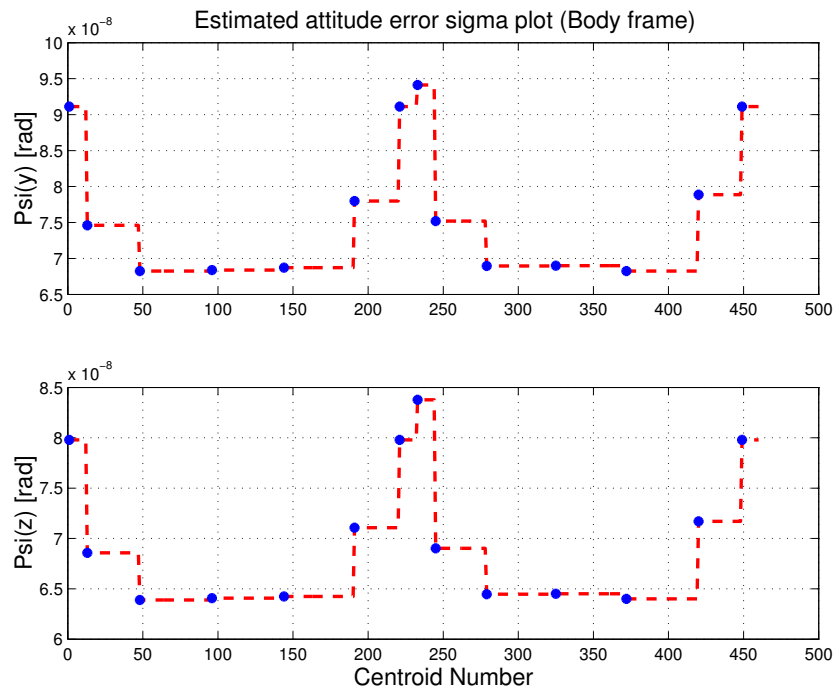


Figure 3.40: Estimated attitude error sigma plot (Body frame)

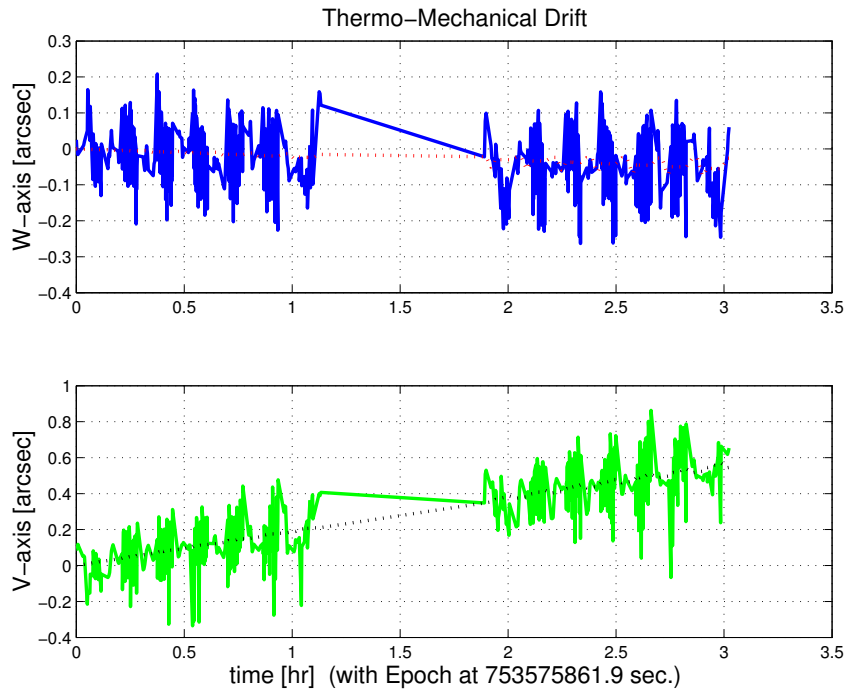


Figure 3.41: Thermo-mechanical boresight drift (equiv. angle in (W,V) coords)

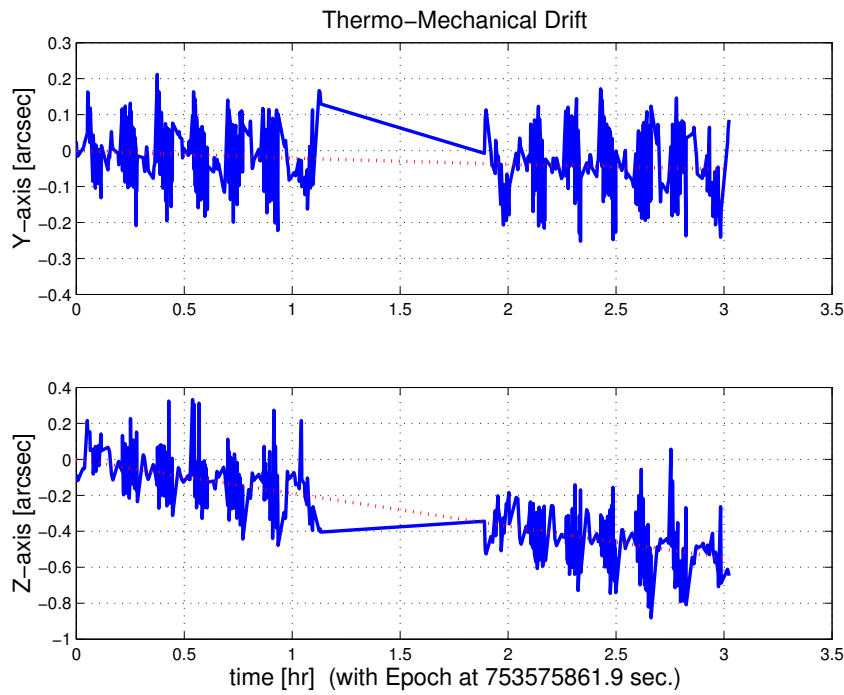


Figure 3.42: Thermo-mechanical boresight drift (equiv. angle in Body frame)

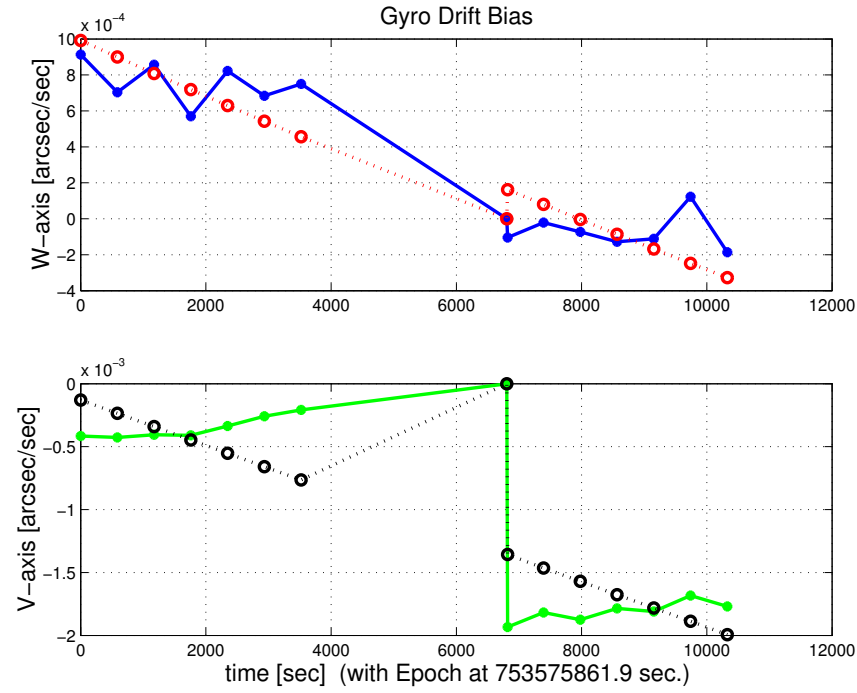


Figure 3.43: Gyro drift bias contribution (equiv. rate in (W,V) coords)

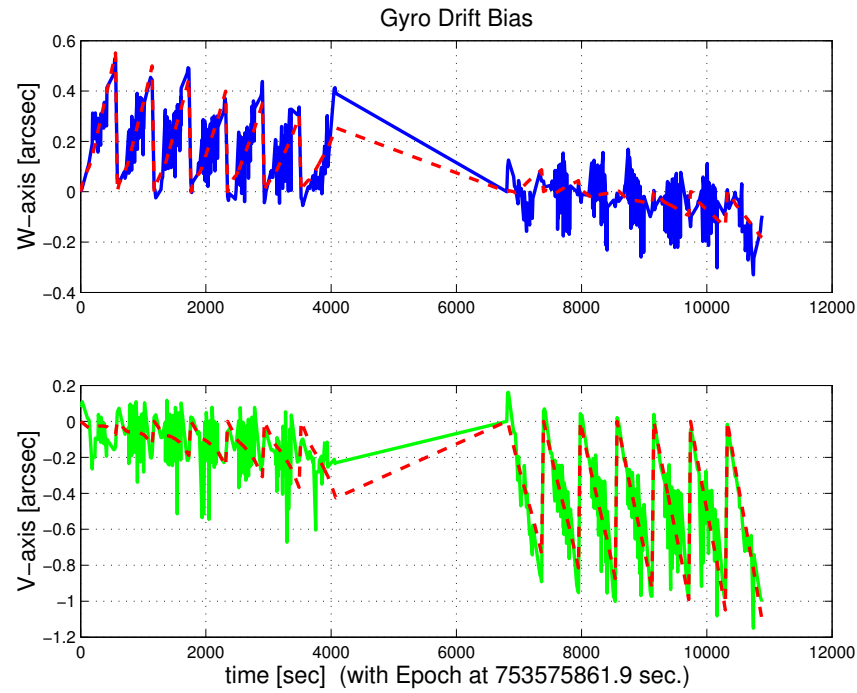


Figure 3.44: Gyro drift bias contribution (equiv. angle in (W,V) coords)

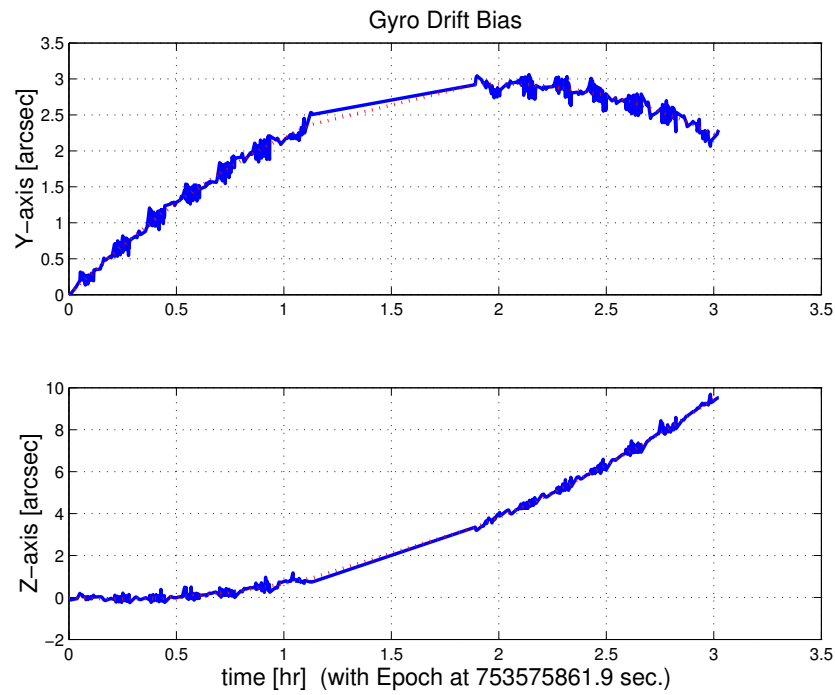


Figure 3.45: Gyro drift bias contribution (equiv. angle in Body frame)

### 3.2 IPF OUTPUT DATA (IF MINI FILE)

OUTPUT FILE NAME: IFmini602095.dat DATE: 02-Dec-2003 TIME: 19:18  
 INSTRUMENT NAME: MIPS\_24um\_center NF: 95  
 IPF FILTER VERSION: IPF.V3.0.OB SW RELEASE DATE: November 3, 2003  
 FRAME TABLE USED: BodyFrames\_FTU\_14a

---

----- IPF BROWN ANGLE SUMMARY -----

WAS			IS			
Frame Number	theta_Y (arcmin)	theta_Z (arcmin)	angle (deg)	theta_Y (arcmin)	theta_Z (arcmin)	angle (deg)
095	+6.716105	+4.246060	+0.637930	+6.721826	+4.243820	+0.628212
096	+6.695190	+7.060913	+0.637930	+6.703859	+7.055562	+0.628212
099	+7.756798	+4.259313	+0.637930	+7.762937	+4.257169	+0.628212
100	+5.659609	+4.234140	+0.637930	+5.665074	+4.231696	+0.628212
103	+6.819955	+4.247316	+0.637930	+6.825711	+4.245090	+0.628212
104	+6.633060	+4.245067	+0.637930	+6.638755	+4.242815	+0.628212

---

OFFSET	NF	Delta_CW	Delta_CV
0	95	+0.000	+0.000 pixels

OFFSET FRAME NAME: MIPS\_24um\_center

Brown Angle	theta_Y(arcmin)	theta_Z(arcmin)	angle(deg)
WAS(FTB)	+6.716105	+4.246060	+0.637930
IS (EST)	+6.721826	+4.243820	+0.628212
dT_EST	+0.005721	-0.002240	-0.009717
T_sSIGMA	+0.000268	+0.000261	+0.002879
dT_EST/T_sSIGMA	+21.373226	-8.591985	-3.375556

---

OFFSET	NF	Delta_CW	Delta_CV
1	96	+0.000	-64.000 pixels

OFFSET FRAME NAME: MIPS\_24um\_plusY\_edge

Brown Angle	theta_Y(arcmin)	theta_Z(arcmin)	angle(deg)
WAS(FTB)	+6.695190	+7.060913	+0.637930
IS (EST)	+6.703859	+7.055562	+0.628212
dT_EST	+0.008670	-0.005350	-0.009717
T_sSIGMA	+0.000390	+0.000383	+0.002879
dT_EST/T_sSIGMA	+22.245672	-13.953343	-3.375558

---

OFFSET	NF	Delta_CW	Delta_CV
2	99	+25.000	+0.000 pixels

OFFSET FRAME NAME: MIPS\_24um\_small\_FOV1

Brown Angle	theta_Y(arcmin)	theta_Z(arcmin)	angle(deg)
WAS(FTB)	+7.756798	+4.259313	+0.637930
IS (EST)	+7.762937	+4.257169	+0.628212
dT_EST	+0.006139	-0.002144	-0.009717
T_sSIGMA	+0.000255	+0.000251	+0.002879
dT_EST/T_sSIGMA	+24.118740	-8.550594	-3.375557

---

OFFSET	NF	Delta_CW	Delta_CV
3	100	-25.500	+0.000 pixels

OFFSET FRAME NAME: MIPS\_24um\_small\_FOV2

Brown Angle	theta_Y(arcmin)	theta_Z(arcmin)	angle(deg)
WAS(FTB)	+5.659609	+4.234140	+0.637930
IS (EST)	+5.665074	+4.231696	+0.628212
dT_EST	+0.005465	-0.002444	-0.009717
T_sSIGMA	+0.000258	+0.000246	+0.002879
dT_EST/T_sSIGMA	+21.179236	-9.944902	-3.375556

---

OFFSET	NF	Delta_CW	Delta_CV
4	103	+2.500	+0.000 pixels

OFFSET FRAME NAME: MIPS\_24um\_large\_FOV1

Brown Angle	theta_Y(arcmin)	theta_Z(arcmin)	angle(deg)
WAS(FTB)	+6.819955	+4.247316	+0.637930
IS (EST)	+6.825711	+4.245090	+0.628212

dT_EST	+0.005755	-0.002225	-0.009717
T_sSIGMA	+0.000267	+0.000261	+0.002879
dT_EST/T_sSIGMA	+21.528771	-8.536610	-3.375556

OFFSET	NF	Delta_CW	Delta_CV
5	104	-2.000	+0.000 pixels
OFFSET FRAME NAME: MIPS_24um_large_FOV2			
Brown Angle	theta_Y(arcmin)	theta_Z(arcmin)	angle(deg)
WAS(FTB)	+6.633060	+4.245067	+0.637930
IS (EST)	+6.638755	+4.242815	+0.628212
dT_EST	+0.005695	-0.002252	-0.009717
T_sSIGMA	+0.000268	+0.000260	+0.002879
dT_EST/T_sSIGMA	+21.269327	-8.646350	-3.375556

VARNAME	MEAN	SIGMA	SCALED_SIGMA
a00	-1.5877962194911865E-004	+5.6074167712169990E-005	+5.3006527472556519E-005
b00	-2.1263046444906114E-004	+7.8358920515259108E-005	+7.4072151981499629E-005
c00	-1.1905880467921641E-003	+4.9209568729192622E-005	+4.6517468973337786E-005
a10	+4.5903737071241908E+000	+2.0395174313832184E-001	+1.9279418878277785E-001
b10	+4.4617004892088712E+000	+2.8099692687996636E-001	+2.6562447437154285E-001
c10	+1.1012184796910059E+001	+2.8359172768657320E-001	+2.6807732183861932E-001
d10	-1.1496388061253342E+000	+2.1147192429963435E-001	+1.9990296463428639E-001
a01	+8.0348888827276834E+000	+1.3175140408091843E-001	+1.2454370175961439E-001
b01	+4.2815218751340707E+000	+1.7711292169398987E-001	+1.6742363431423132E-001
c01	-1.6160111270247537E+001	+1.1506208563998141E-001	+1.0876740310853740E-001
d01	-2.218116354195640E+000	+1.3724961133427385E-001	+1.2974111949608025E-001
e01	-1.8377235746694279E+001	+1.7688354552245991E-001	+1.6720680658706538E-001
f01	+2.5538655928081306E+000	+1.1794872495709381E-001	+1.1149612352488469E-001
del_alpha	+7.1143720255240073E-015	+1.2847549721851603E-004	+1.2144700939333995E-004
beta	+9.6245187272690003E-001	+1.7581747981171902E-004	+1.6619906195723872E-004
del_theta1	+9.6141966458331007E-016	+5.3151343703491090E-005	+5.0243601914593024E-005
del_theta2	-1.5603988014759517E-017	+8.2370910167444326E-008	+7.7864658377845363E-008
del_theta3	+3.5243250916405872E-017	+8.0211236041361491E-008	+7.5823133187786526E-008
del_arx	+1.5623678354409628E-015	+2.4776239600526897E-005	+2.3420809949301143E-005
del_ary	-4.207474944734255E-017	+3.0681155223482390E-006	+2.9002686327706794E-006
del_arz	-1.1738671810751582E-015	+3.0681857927507649E-006	+2.9003350589018905E-006
brx	+2.9421592405881364E-009	+1.1538411250927114E-008	+1.0907181290703011E-008
bry	-3.1320304641419534E-011	+1.5922196187313966E-009	+1.5051143227991598E-009
brz	-2.5802469792405801E-010	+1.5921891958286359E-009	+1.5050855642371201E-009
crx	+1.8544221606750087E-013	+2.0995923696022888E-012	+1.9847303163153257E-012
cry	+1.5212057531472766E-015	+3.0385184062373355E-013	+2.8722906812067090E-013
crz	+2.2293489250348535E-015	+3.0384612246206422E-013	+2.8722366278152838E-013
bgx	+6.2759586801008147E-007	+2.8475896072888197E-007	+2.6918069925550047E-007
bgy	+3.9152123197429447E-009	+1.6456622955760336E-009	+1.5556333199408221E-009
bgz	-7.8330759269850663E-010	+1.6707868865384356E-009	+1.5793834240515295E-009
cgx	-3.0696507710504126E-011	+4.3010187614752133E-011	+4.0657236378496812E-011
cgy	-5.3912015596375150E-013	+3.0983230363704284E-013	+2.9288235893081316E-013
cgz	+9.3212433996922011E-013	+3.1358857631406815E-013	+2.9643313781836040E-013

LSQF RESIDUAL SIGMA SCALE = +9.4529316502101757E-001

	a_mirror(1)	a_mirror(2)	a_mirror(3)	qT(1)	qT(2)	qT(3)	qT(4)	
a_mirror_ipf	+0.000000000000000E+000	+1.2565262419800743E-002	+9.9992105397392328E-001	FrmTbl:	+5.5663503708387003E-003	-9.8024034448415199E-004	-6.1211659772710003E-004	+9.9998383996226903E-001
a_mirror_tpf	-1.9533180461764328E-003	+1.6036329010015136E-003	+9.9999680644996536E-001	Estim:	+5.4815514672171411E-003	-9.8101874430645648E-004	-6.1186942720066104E-004	+9.9998430778264702E-001
beta	beta_0	beta	beta_total	DelTheta	deltheta(1)	deltheta(2)	deltheta(3)	
	+2.8047410000000001E-006	+9.6245187272690003E-001	+2.6994282279639184E-006		-1.6959883788282226E-004	-1.6568624849575081E-006	+6.6995859420394391E-007	[rad]
EulAngT	theta(1)	theta(2)	theta(3)	Mean	+1.0964372052345999E-002	-1.9552999582975726E-003	-1.2344773340676166E-003	[rad]

```

SigmaT      +5.3151343703491090E-005  +8.2370910167444326E-008  +8.0211236041361491E-008
-----
qR          qR(1)                  qR(2)                  qR(3)                  qR(4)
ASFILE:    +7.0908659836277366E-004  +1.2693941826000810E-003  -1.6274217341560870E-004  +9.9999892711639404E-001
Estim:     +6.7021401262892203E-004  +1.2690468333789351E-003  -1.6213404774591299E-004  +9.9999895702238750E-001
DelThetaR   delthetaR(1)            delthetaR(2)            delthetaR(3)            [rad]
          -7.7746561927139013E-005  -7.0652015109420104E-007  +1.1180905698580830E-006
EulAngR    angR(1)                angR(2)                angR(3)                [rad]
Mean       +1.3400198337425455E-003  +2.5383110743363848E-003  -3.2256773609560835E-004
SigmaR     +2.4776239600526897E-005  +3.0681155223482390E-006  +3.0681857927507649E-006
-----
Initial Gyro Bias   Bg0(1)                  Bg0(2)                  Bg0(3)
          -4.3628790535876760E-007  -2.0367018294109582E-007  +3.6563167782333039E-007
Gyro Bias Correction Bg(1)                  Bg(2)                  Bg(3)
          +6.2759586801008147E-007  +3.9152123197429447E-009  -7.8330759269850663E-010
Total Gyro Bias     BgT(1)                 BgT(2)                 BgT(3)
          +1.9130796265131386E-007  -1.9975497062135288E-007  +3.6484837023063188E-007
-----
Initial Gyro Bias Rate   Cg0(1)                  Cg0(2)                  Cg0(3)
          +0.0000000000000000E+000  +0.0000000000000000E+000  +0.0000000000000000E+000
Gyro Bias Rate Correction Cg(1)                  Cg(2)                  Cg(3)
          -3.0696507710504126E-011  -5.3912015596375150E-013  +9.3212433996922011E-013
Total Gyro Bias Rate     CgT(1)                 CgT(2)                 CgT(3)
          -3.0696507710504126E-011  -5.3912015596375150E-013  +9.3212433996922011E-013
-----
OFFSET        NF      Delta_CW      Delta_CV
1             96      +0.000      -64.000      pixels
OFFSET FRAME NAME: MIPS_24um_plusY_edge
qT          qT(1)                  qT(2)                  qT(3)                  qT(4)
WAS(FTB)    +5.5659517308697505E-003  -9.7947717279747932E-004  -1.0215305487940502E-003  +9.9998350850458306E-001
IS (EST)    +5.4811525155637935E-003  -9.8064719308595767E-004  -1.0208285619320086E-003  +9.9998397647523896E-001
DelTheta   deltheta(1)            deltheta(2)            deltheta(3)
Units       rad                  rad                  rad
          -1.6959707968843197E-004  -2.5043864469100749E-006  +1.5842613813359985E-006
EulAngT    theta(1)              theta(2)              theta(3)              [rad]
Mean       +1.0964372052346001E-002  -1.9500735611944968E-003  -2.0523799062172440E-003
sSigmaT    +5.0243584669836031E-005  +1.1336452140473540E-007  +1.1153477724036373E-007
SigmaT     +5.3151325460730394E-005  +1.1992525239745584E-007  +1.1798961567429071E-007
-----
OFFSET        NF      Delta_CW      Delta_CV
2             99      +25.000      +0.000      pixels
OFFSET FRAME NAME: MIPS_24um_small_FOV1
qT          qT(1)                  qT(2)                  qT(3)                  qT(4)
WAS(FTB)    +5.5662538280227556E-003  -1.1316112973882811E-003  -6.1320141015468849E-004  +9.9998367999594084E-001
IS (EST)    +5.4814549312274070E-003  -1.1324503853494595E-003  -6.1298068602793580E-004  +9.9998414760567089E-001
DelTheta   deltheta(1)            deltheta(2)            deltheta(3)
Units       rad                  rad                  rad
          -1.6959870359077350E-004  -1.7785760671188138E-006  +6.4342528376222883E-007
EulAngT    theta(1)              theta(2)              theta(3)              [rad]
Mean       +1.0964372052346001E-002  -2.2581467337236217E-003  -1.2383603629807604E-003
sSigmaT    +5.0243598944541018E-005  +7.4034943636926656E-008  +7.2928823032608489E-008
SigmaT     +5.3151340561553628E-005  +7.8319558816740800E-008  +7.7149423830846171E-008
-----
OFFSET        NF      Delta_CW      Delta_CV
3             100      -25.500      +0.000      pixels
OFFSET FRAME NAME: MIPS_24um_small_FOV2
qT          qT(1)                  qT(2)                  qT(3)                  qT(4)
WAS(FTB)    +5.5664474678460652E-003  -8.2657205344854390E-004  -6.1123845851204566E-004  +9.9998397878604794E-001
IS (EST)    +5.4816485521974280E-003  -8.2731316353717825E-004  -6.1094873711210350E-004  +9.9998444679090903E-001
DelTheta   deltheta(1)            deltheta(2)            deltheta(3)
Units       rad                  rad                  rad
          -1.6959894022143765E-004  -1.5818002527745599E-006  +7.2857530851818151E-007

```

```

EulAngT      theta(1)          theta(2)          theta(3)          [rad]
Mean        +1.0964372052345999E-002 -1.6479033256415350E-003 -1.2309505320464277E-003
sSigmaT     +5.0243600215834255E-005 +7.5064747437668726E-008 +7.1485849787101995E-008
SigmaT      +5.3151341906420263E-005 +7.9408960326080163E-008 +7.5622941572324373E-008
-----
OFFSET      NF       Delta_CW       Delta_CV
4           103      +2.500      +0.000      pixels
OFFSET FRAME NAME: MIPS_24um_large_FOV1
qT          qT(1)          qT(2)          qT(3)          qT(4)
WAS(FTB)   +5.5663407785030133E-003 -9.9534554975494265E-004 -6.1221510359754845E-004 +9.9998382503430572E-001
IS (EST)   +5.4815418756747926E-003 -9.9612894331162585E-004 -6.1197125806448135E-004 +9.9998429283512880E-001
DelTheta    deltheta(1)      deltheta(2)      deltheta(3)
Units       rad            rad            rad
EulAngT    theta(1)          theta(2)          theta(3)          [rad]
Mean        +1.0964372052345999E-002 -1.9855188063244685E-003 -1.2348466843772731E-003
sSigmaT     +5.0243601825243293E-005 +7.7765734904140290E-008 +7.5829670560737365E-008
SigmaT      +5.3151343608970432E-005 +8.2266261707722442E-008 +8.0218151750892407E-008
-----
OFFSET      NF       Delta_CW       Delta_CV
5           104      -2.000      +0.000      pixels
OFFSET FRAME NAME: MIPS_24um_large_FOV2
qT          qT(1)          qT(2)          qT(3)          qT(4)
WAS(FTB)   +5.5663580350760848E-003 -9.6816128275258886E-004 -6.1203938908990752E-004 +9.9998385173448789E-001
IS (EST)   +5.4815591307850508E-003 -9.6893585960022605E-004 -6.1178944971230186E-004 +9.9998431957029466E-001
DelTheta    deltheta(1)      deltheta(2)      deltheta(3)
Units       rad            rad            rad
EulAngT    theta(1)          theta(2)          theta(3)          [rad]
Mean        +1.0964372052345999E-002 -1.9311354127426405E-003 -1.2341848862309360E-003
sSigmaT     +5.0243601953021452E-005 +7.7885823558244389E-008 +7.5754768032588598E-008
SigmaT      +5.3151343744143481E-005 +8.2393300237723269E-008 +8.0138914397952165E-008
-----
q(1)          q(2)          q(3)          q(4)
PCRS1A: +5.3371888965461637E-007 +3.744233778550031E-004 -1.4253684912431913E-003 +9.9999891405806784E-001
PCRS2A: -5.2779261998836216E-007 +3.8462959425181312E-004 +1.3722087221825403E-003 +9.9999898455099423E-001
*****
CS-FILE PARAMETERS: ***** AS-FILE PARAMETERS: *****
Row (01) PIX2RADX: +1.2087416876100000E-005 Row (1) TASTART: +7.5357550039074707E+008
Row (02) PIX2RADY: +1.2595908372599999E-005 Row (2) TASTOP: +7.5358749929079282E+008
Row (03) CX0: +6.450000000000000E+001 Row (3) S/C TIME: +7.5355685689079285E+008
Row (04) CY0: +6.450000000000000E+001 Row (4) QR1: +7.0908659836277366E-004
Row (05) BETA0: +2.8047410000000001E-006 Row (5) QR2: +1.2693941826000810E-003
Row (06) GAMMA_E0: +2.007000000000000E+003 Row (6) QR3: -1.6274217341560870E-004
Row (07) D11: -1.000000000000000E+000 Row (7) QR4: +9.9999892711639404E-001
Row (08) D12: +0.000000000000000E+000
Row (09) D21: +0.000000000000000E+000
Row (10) D22: -1.000000000000000E+000
Row (11) DG: -1.000000000000000E+000
-----
INITIAL STA-TO-PCRS ALIGNMENT (R) KNOWLEDGE (1-SIGMA)
SIGMA(X)      SIGMA(Y)      SIGMA(Z)
5.07582033E+000 3.78025944E-001 3.78557885E-001 [arcsec]
-----
PIX2RADX = 1.208741687610E-005 [rad/pixel]
XPIXSIZE = 2.4932 [arcsec]
PIX2RADY = 1.259590837260E-005 [rad/pixel]
YPIXSIZE = 2.5981 [arcsec]
CX0 = 64.5 [pixel] = 160.81 [arcsec]
CY0 = 64.5 [pixel] = 167.58 [arcsec]
-----
NOMINAL BETA0 = 2.804741000000E-006 [rad/encoder unit]

```

```

ENCODER UNIT SIZE = 0.58[arcsec]
GAMMA_EO = 2007.00[encoder unit] = 1161.09[arcsec]
-----
| -1 | +0 |
FLIP MATRIX D = |----|----| and DG = -1
| +0 | -1 |
-----

```

### 3.3 IPF EXECUTION LOG

```

*****
IPF EXECUTION-LOG FILE NAME: LG602095.dat
INSTRUMENT TYPE: MIPS_24um_center
IPF FILTER EXECUTION DATE: 02-Dec-2003 TIME: 19:12
IPF FILTER VERSION USED: IPF.V3.0.0B
*****


----- Loading & Preparing Input Files -----
AAFILE: AA601095 Loaded! AAFILE dimension = 119990 X 21
ASFILE: AS601095 Loaded!
CAFILe: CA901095 Loaded! CAFILe dimension = 460 X 15
CBFILE: CB601095 Loaded! CBFILE dimension = 126 X 15
CCFILE: CC602095 Created! CCFILE dimension = 586 X 19
CSFILE: CS601095 Loaded!
Loading Input Files Completed!
-----


----- Selected Mask Vectors -----
index = 1 2 3 4 5 6 7 8 9 10 11 12 13 14 15 16 17 18 19 20
-----
mask1 = [ 1 1 1 1 1 1 1 0 0 0 0 1 1 1 1 1 1 1 ]
mask2 = [ 1 1 1 1 1 1 1 1 1 1 1 1 1 1 1 1 1 1 ]
-----


----- Selected Initial Gyro Bias Parameters -----
User Entered 1 : Use AFILe database - from S/C filter
IPF Linearized Using Nominal Gyro Bias Estimates
bg0 = [-4.3628790535876760E-007 -2.0367018294109582E-007 +3.6563167782333039E-007 ]
cg0 = [+0.0000000000000000E+000 +0.0000000000000000E+000 +0.0000000000000000E+000 ]
-----


----- Gyro Pre-Processor Run Completed -----
AGFILE CREATED: AG602095.m ACFILe CREATED: AC602095.m
-----


Total Gyro Preprocessor Execution Time: 81 seconds

FRAME TABLE ENTRIES FOR PCRS LOADED TO TPCRS
q_PCRS4 = [ +5.3371888965461637E-007 q_PCRS5 = [ +7.3379987833742897E-007
+3.7444233778550031E-004 +5.2236196154513707E-004
-1.4253684912431913E-003 -1.4047712280184723E-003
+9.9999891405806784E-001 ]; +9.9999887687698918E-001 ];
q_PCRS8 = [ -5.2779261998836216E-007 q_PCRS9 = [ -7.1963421681856818E-007
+3.8462959425181312E-004 +5.3239763239987400E-004
+1.3722087221825403E-003 +1.3516841804518383E-003
+9.9999898455099423E-001 ]; +9.9999894475050310E-001 ];
----- Initial Conditions for State ----- ----- Initial Square-Root Cov (diag) -----
p1(01) = a00 = +0.0000000000000000E+000 Sigma_initial(01,01) = 1.0000000000000000E+000
p1(02) = b00 = +0.0000000000000000E+000 Sigma_initial(02,02) = 1.0000000000000000E+000
p1(03) = c00 = +0.0000000000000000E+000 Sigma_initial(03,03) = 1.0000000000000000E+000
-----
```

```

p1(04) = a10 = +0.0000000000000000E+000 Sigma_initial(04,04) = 1.0000000000000000E+002
p1(05) = b10 = +0.0000000000000000E+000 Sigma_initial(05,05) = 1.0000000000000000E+002
p1(06) = c10 = +0.0000000000000000E+000 Sigma_initial(06,06) = 1.0000000000000000E+002
p1(07) = d10 = +0.0000000000000000E+000 Sigma_initial(07,07) = 1.0000000000000000E+002
p1(08) = a20 = +0.0000000000000000E+000 Sigma_initial(08,08) = 9.9999000000000000E+004
p1(09) = b20 = +0.0000000000000000E+000 Sigma_initial(09,09) = 9.9999000000000000E+004
p1(10) = c20 = +0.0000000000000000E+000 Sigma_initial(10,10) = 9.9999000000000000E+004
p1(11) = d20 = +0.0000000000000000E+000 Sigma_initial(11,11) = 9.9999000000000000E+004
p1(12) = a01 = +0.0000000000000000E+000 Sigma_initial(12,12) = 1.0000000000000000E+004
p1(13) = b01 = +0.0000000000000000E+000 Sigma_initial(13,13) = 1.0000000000000000E+004
p1(14) = c01 = +0.0000000000000000E+000 Sigma_initial(14,14) = 1.0000000000000000E+004
p1(15) = d01 = +0.0000000000000000E+000 Sigma_initial(15,15) = 1.0000000000000000E+004
p1(16) = e01 = +0.0000000000000000E+000 Sigma_initial(16,16) = 1.0000000000000000E+004
p1(17) = f01 = +0.0000000000000000E+000 Sigma_initial(17,17) = 1.0000000000000000E+004
-----
p2f(01) = am1 = +0.0000000000000000E+000 Sigma_initial(18,18) = 1.0000000000000001E-001
p2f(02) = am2 = +0.0000000000000000E+000 Sigma_initial(19,19) = 1.0000000000000001E-001
p2f(03) = am3 = +1.0000000000000000E+000 Sigma_initial(20,20) = 1.0000000000000001E-001
p2f(04) = beta = +1.0000000000000000E+000 Sigma_initial(21,21) = 1.0000000000000000E-002
p2f(05) = qT1 = +5.5663503708387055E-003 Sigma_initial(22,22) = 1.0000000000000000E-002
p2f(06) = qT2 = -9.8024034448415285E-004 Sigma_initial(23,23) = 2.4608271387666178E-004
p2f(07) = aT3 = -6.1211659772710057E-004 Sigma_initial(24,24) = 1.8327214933301909E-005
p2f(08) = qT4 = +9.9998383996226992E-001 Sigma_initial(25,25) = 1.8353004197221061E-005
p2f(09) = qR1 = +7.0908659836277366E-004 Sigma_initial(26,26) = 9.1882207525891937E-005
p2f(10) = qR2 = +1.2693941826000810E-003 Sigma_initial(27,27) = 9.1882207525891937E-005
p2f(11) = qR3 = -1.6274217341560870E-004 Sigma_initial(28,28) = 9.1882207525891937E-005
p2f(12) = qR4 = +9.9999892711639404E-001 Sigma_initial(29,29) = 8.4423400598310735E-009
p2f(13) = brx = +0.0000000000000000E+000 Sigma_initial(30,30) = 8.4423400598310735E-009
p2f(14) = bry = +0.0000000000000000E+000 Sigma_initial(31,31) = 8.4423400598310735E-009
p2f(15) = brz = +0.0000000000000000E+000 Sigma_initial(32,32) = 9.1882207525891937E-005
p2f(16) = crx = +0.0000000000000000E+000 Sigma_initial(33,33) = 9.1882207525891937E-005
p2f(17) = cry = +0.0000000000000000E+000 Sigma_initial(34,34) = 9.1882207525891937E-005
p2f(18) = crz = +0.0000000000000000E+000 Sigma_initial(35,35) = 8.4423400598310735E-009
p2f(19) = bgx = +0.0000000000000000E+000 Sigma_initial(36,36) = 8.4423400598310735E-009
p2f(20) = bgy = +0.0000000000000000E+000 Sigma_initial(37,37) = 8.4423400598310735E-009
p2f(21) = bgz = +0.0000000000000000E+000 Sigma_initial(38,38) = 8.4423400598310735E-009
p2f(22) = cgx = +0.0000000000000000E+000 Sigma_initial(39,39) = 8.4423400598310735E-009
p2f(23) = cgy = +0.0000000000000000E+000 Sigma_initial(40,40) = 8.4423400598310735E-009
p2f(24) = cgz = +0.0000000000000000E+000 Sigma_initial(41,41) = 8.4423400598310735E-009
-----
```

```

----- IPF KALMAN FILTER STARTED -----
Iteration#001: |dp|= +2.931688443113E+001 RMS(|Res|)=+1.312466543613E-005
Iteration#002: |dp|= +2.792118043707E-002 RMS(|Res|)=+3.187499974732E-006
Iteration#003: |dp|= +1.407678989580E-003 RMS(|Res|)=+8.739623074335E-007
Iteration#004: |dp|= +3.562101747727E-005 RMS(|Res|)=+8.653792127574E-007
Iteration#005: |dp|= +4.920224615036E-006 RMS(|Res|)=+8.654436226827E-007
Iteration#006: |dp|= +3.509608381056E-007 RMS(|Res|)=+8.654274024816E-007
Iteration#007: |dp|= +4.083383751390E-008 RMS(|Res|)=+8.654251881073E-007
Iteration#008: |dp|= +4.612615243796E-009 RMS(|Res|)=+8.654254783712E-007
Iteration#009: |dp|= +4.689038022258E-010 RMS(|Res|)=+8.654255587541E-007
Iteration#010: |dp|= +3.900892992912E-010 RMS(|Res|)=+8.654255555252E-007
Iteration#011: |dp|= +2.227629607895E-010 RMS(|Res|)=+8.654255530680E-007
Iteration#012: |dp|= +3.983523447278E-011 RMS(|Res|)=+8.654255530246E-007
Iteration#013: |dp|= +1.531989117596E-010 RMS(|Res|)=+8.654255530969E-007
Iteration#014: |dp|= +1.901053758388E-010 RMS(|Res|)=+8.654255530983E-007
Iteration#015: |dp|= +1.167043780404E-010 RMS(|Res|)=+8.654255530881E-007
Iteration#016: |dp|= +2.127068639119E-010 RMS(|Res|)=+8.654255530877E-007
Iteration#017: |dp|= +1.795147899522E-010 RMS(|Res|)=+8.654255530987E-007
Iteration#018: |dp|= +1.101381020253E-010 RMS(|Res|)=+8.654255530964E-007
Iteration#019: |dp|= +5.545373125133E-010 RMS(|Res|)=+8.654255530888E-007
Iteration#020: |dp|= +1.726548561226E-010 RMS(|Res|)=+8.654255530961E-007
Iteration#021: |dp|= +5.595079162538E-010 RMS(|Res|)=+8.654255530937E-007
Iteration#022: |dp|= +2.865394193017E-010 RMS(|Res|)=+8.654255531079E-007
Iteration#023: |dp|= +1.300212764247E-010 RMS(|Res|)=+8.654255530933E-007
Iteration#024: |dp|= +4.181617924385E-010 RMS(|Res|)=+8.654255530982E-007
Iteration#025: |dp|= +2.722229504306E-010 RMS(|Res|)=+8.654255530947E-007
IPF Kalman Filter Completed with Error |dp1| + |dp2| = +2.7222295043063589E-010
```

---

----- IPF LEAST SQUARES FILTER STARTED -----

```

Iteration#001 COND#=+3.275615343400E+009, |dp|=+2.931682590468E+001
Iteration#002 COND#=+3.275611935260E+009, |dp|=+2.819689078444E-002
Iteration#003 COND#=+3.275611898185E+009, |dp|=+1.145539518074E-003
Iteration#004 COND#=+3.275611900129E+009, |dp|=+2.863872747440E-005
Iteration#005 COND#=+3.275611899121E+009, |dp|=+3.803407553147E-007
Iteration#006 COND#=+3.275611898413E+009, |dp|=+4.851678447718E-009
Iteration#007 COND#=+3.275611900162E+009, |dp|=+6.528415908106E-011
Iteration#008 COND#=+3.275611900128E+009, |dp|=+3.620461227759E-011
Iteration#009 COND#=+3.275611900236E+009, |dp|=+2.013070754749E-011
Iteration#010 COND#=+3.275611900500E+009, |dp|=+3.230308055604E-011
Iteration#011 COND#=+3.275611901416E+009, |dp|=+4.005494532998E-011
Iteration#012 COND#=+3.275611900096E+009, |dp|=+3.053126443405E-011
Iteration#013 COND#=+3.275611901001E+009, |dp|=+4.283235833126E-011
Iteration#014 COND#=+3.275611899785E+009, |dp|=+4.871370271768E-011
Iteration#015 COND#=+3.275611899899E+009, |dp|=+2.884653040892E-011
Iteration#016 COND#=+3.275611899660E+009, |dp|=+1.544446910479E-011
Iteration#017 COND#=+3.275611900831E+009, |dp|=+2.768188600431E-011
Iteration#018 COND#=+3.275611900269E+009, |dp|=+3.132786640245E-011
Iteration#019 COND#=+3.275611899913E+009, |dp|=+3.981586914644E-011
Iteration#020 COND#=+3.275611900422E+009, |dp|=+3.304350752015E-011
Iteration#021 COND#=+3.275611900758E+009, |dp|=+2.564746965544E-011
Iteration#022 COND#=+3.275611900102E+009, |dp|=+2.200455082532E-011
Iteration#023 COND#=+3.275611900910E+009, |dp|=+3.257997621227E-011
Iteration#024 COND#=+3.275611900664E+009, |dp|=+4.400277971364E-011
Iteration#025 COND#=+3.275611898602E+009, |dp|=+3.971705140677E-011
IPF Least Squares Filter Completed with Error |dp1| + |dp2| = +3.9717051406769921E-011
-----
```

Total Execution Time: 359 seconds

## 4 COMMENTS

Overall the data looked clean, and the filter converged nicely.

Comments:

1. The run was performed in normal IPF operating mode.
2. There were 15 sandwich maneuvers with 460 science centroids (7 centroids were removed from the original 467 centroids, at the 3-sigma level) and 126 PCRS measurements.
3. We estimated 33 parameters consisting of: 3 constant and 6 linear plate scales, 4 Gamma Dependent parameters, 2 mirror parameters, 3 IPF alignment angles, 3 STA-to-PCRS alignment angles, 6 STA-to-PCRS thermomechanical drift parameters, and 3 gyro bias and 3 gyro bias-drift parameters.
4. The linear plate scales were helpful in this run to estimate centroids accurately (see quiver plots in Figures 3-33 and 3-34). The constant plate scales were much smaller than the linear terms. The estimated plate scales (constant and linear) are consistent with those obtained earlier from the Coarse Focal Plane Survey results (i.e., run ID101095).
5. The scan mirror parameter estimates indicate that the mirror scan axis is tilted by 0.7 deg and the scan mirror scale factor is off by 4 percent. These values are consistent with those obtained earlier from the Coarse Focal Plane Survey results (i.e., run ID101095).
6. When we compare the recommended Brown angles in the current run (ID602095) to those recommended by the previous Fine Survey run (ID502095) (note - they both are with respect to the same "WAS" angles since ID502095 was not used in any FTU) the runs disagree by 1" in the V direction. This represents a relatively large discrepancy because these Fine Survey runs should be accurate to 0.1" and this disagreement is 10 times larger.  
Looking carefully at the past and current run, we feel that there is strong evidence that the actual frame changed in the V direction by 1" in the last 3 weeks. We did not think that this was possible and want to check further on this matter. One hypothesis is that there was some non-repeatability in the scan mirror Gamma angle on the order of 1".

We recommend updating frames 95, 96, 99, 100, 103 and 104 with the new quaternions listed in the IF file IF602095.dat. This contains adjustments of 0.35 and 0.13 arcseconds in Y and Z, and 0.01 deg in twist (for the prime frame). If the scan mirror is fully repeatable, this fine survey should be accurate to 0.09 arcsecond which satisfies its fine survey requirement of 0.14 arcseconds by a good margin. Note: If there is really a non-repeatability of the scan mirror on the order of 1", then these results should be revisited, and it may not be possible to meet the .14" Fine Survey requirement.

## IPF TEAM CONTACT INFORMATION

IPF Team email	ipf@sirtfweb.jpl.nasa.gov	
David S. Bayard	X4-8208	David.S.Bayard@jpl.nasa.gov (TEAM LEADER)
Dhemetrio Boussalis	X4-3977	boussali@grover.jpl.nasa.gov
Paul Brugarolas	X4-9243	Paul.Brugarolas@jpl.nasa.gov
Bryan H. Kang	X4-0541	Bryan.H.Kang@jpl.nasa.gov
Edward.C.Wong	X4-3053	Edward.C.Wong@jpl.nasa.gov (TASK MANAGER)

## ACKNOWLEDGEMENTS

This work was performed at the Jet Propulsion Laboratory, California Institute of Technology, under contract with the National Aeronautics and Space Administration.

## References

- [1] D.S. Bayard, B.H. Kang, *SIRTF Instrument Pointing Frame Kalman Filter Algorithm*, JPL D-Document D-24809, September 30, 2003.
- [2] B.H. Kang, D.S. Bayard, *SIRTF Instrument Pointing Frame (IPF) Software Description Document and User's Guide*, JPL D-Document D-24808, September 30, 2003.
- [3] D.S. Bayard, B.H. Kang, *SIRTF Instrument Pointing Frame (IPF) Kalman Filter Unit Test Report*, JPL D-Document D-24810, September 30, 2003.
- [4] *Space Infrared Telescope Facility In-Orbit Checkout and Science Verification Mission Plan*, JPL D-Document D-22622, 674-FE-301 Version 1.4, February 8, 2002.
- [5] *Space Infrared Telescope Facility Observatory Description Document*, Lockheed Martin LMMS/P458569, 674-SEIT-300 Version 1.2, November 1, 2002.
- [6] *SIRTF Software Interface Specification for Science Centroid INPUT Files (CAFILER, CS-FILE)*, JPL SOS-SIS-2002, November 18, 2002.
- [7] *SIRTF Software Interface Specification for Inferred Frames Offset INPUT Files (OFILE)*, JPL SOS-SIS-2003, November 18, 2002.
- [8] *SIRTF Software Interface Specification for PCRS Centroid INPUT Files (CBFILE)*, JPL SIS-FES-015, November 18, 2002.
- [9] *SIRTF Software Interface Specification for Attitude INPUT Files (AFILE, ASFILE)*, JPL SIS-FES-014, January 7, 2002.
- [10] *SIRTF Software Interface Specification for IPF Filter Output Files (IFFILE, LGFILE, TARFILE)*, JPL SOS-SIS-2005, November 18, 2002.
- [11] R.J. Brown, *Focal Surface to Object Space Field of View Conversion*. Systems Engineering Report SER No. S20447-OPT-051, Ball Aerospace & Technologies Corp., November 23, 1999.